



Sviluppo di dosimetri con materiali avanzati per radioterapia clinica

M. Bruzzi

University of Florence, Dept. of Physics and Astronomy and INFN Firenze, Italy

Outline



1. Motivation

2. Advanced materials and devices in clinical radiotherapy dosimetry

- epitaxial silicon
- SiC
- polycrystalline diamond
- perovskites PERO2

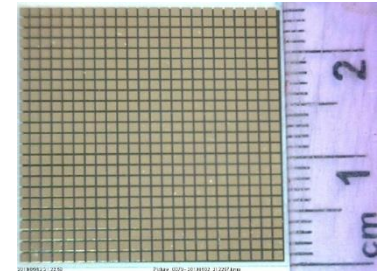
4. Conclusions

Esperimenti finanziati nel corso degli anni da INFN CSN5 presso la sezione di Firenze per lo sviluppo di dosimetri per radioterapia clinica

- **Diamante policristallino**

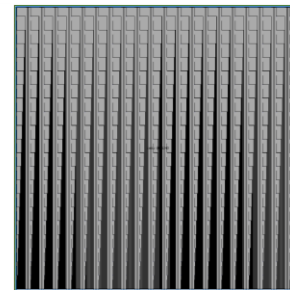
IDDD (96-98) / CANDIDO (99-02) /

DIAPIX (11-13) / IRPT MIUR (14-17) / 3DOSE (17/19)



- **Si ossigenato, SiC, diamante**

CONRAD (03-05)

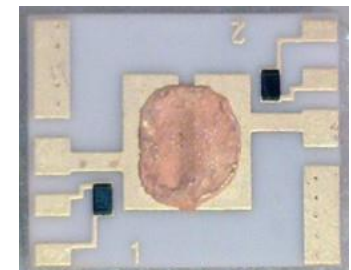


- **Si epitassiale**

PRIMA (04-09)

- **perovskite inorganica**

PERO/PERO2 (19-21)



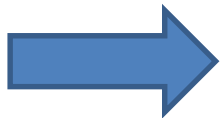
Motivation



Radiotherapy with external beams with high energy (X, γ , electrons, protons, ions) produced by particle accelerators



- immobilization techniques allow for positioning patient during the treatment with always increasing accuracy,
- accelerators equipped with beam modifying devices able to get dose distributions closely shaped on the target volume.



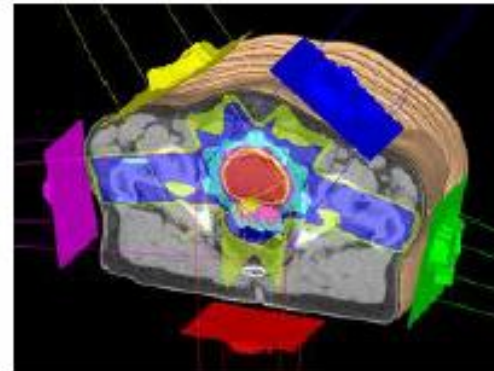
Advanced, highly accurate imaging and dose verifications systems must match with increased accuracy of irradiation techniques

Intensity Modulated Radiation Therapy (IMRT)



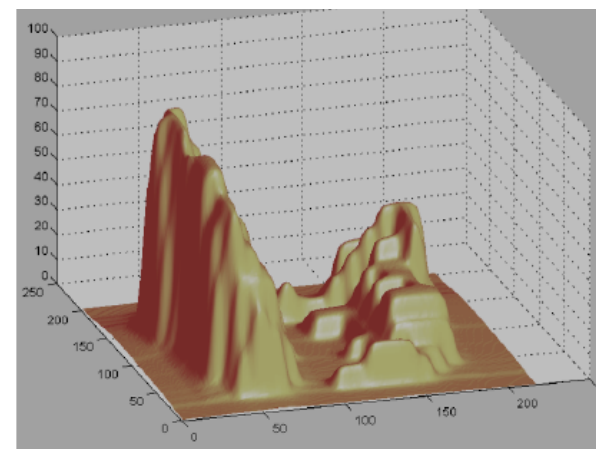
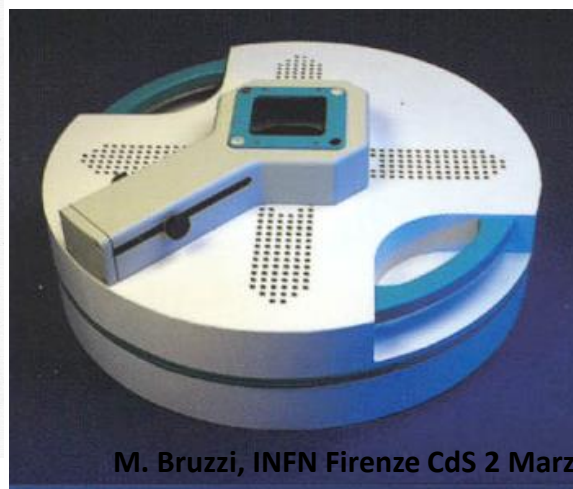
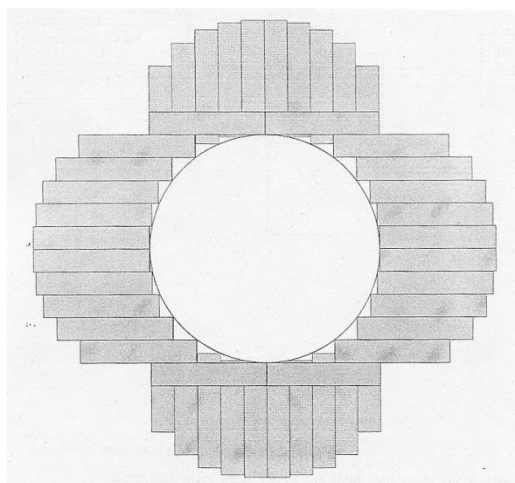
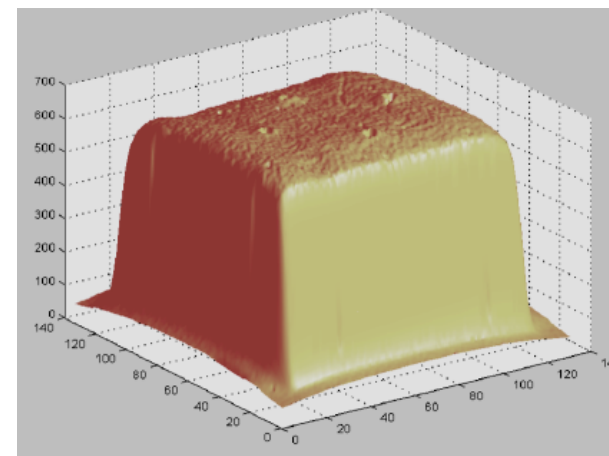
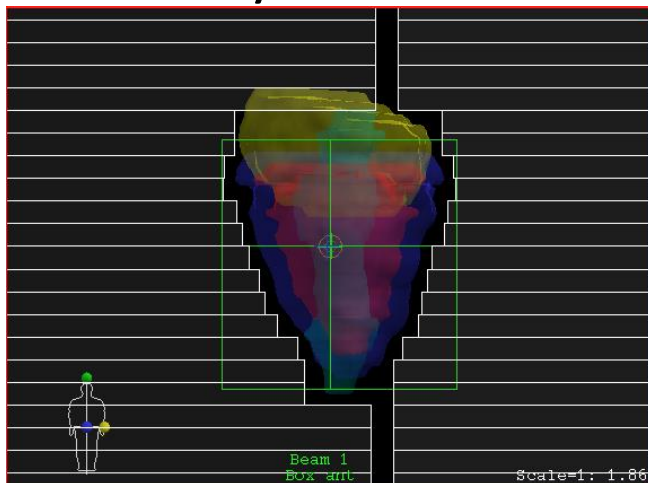
To spare surrounding healthy tissues released dose shaped along an irregular field conformed to the tumor volume

Intensity Modulated Radiation Therapy (IMRT) : a few radiation beams, generally from 2 to 9, produced by the same linear accelerator and directed towards the tumor from different angles, in order to concentrate the dose released on the volume of the tumor.



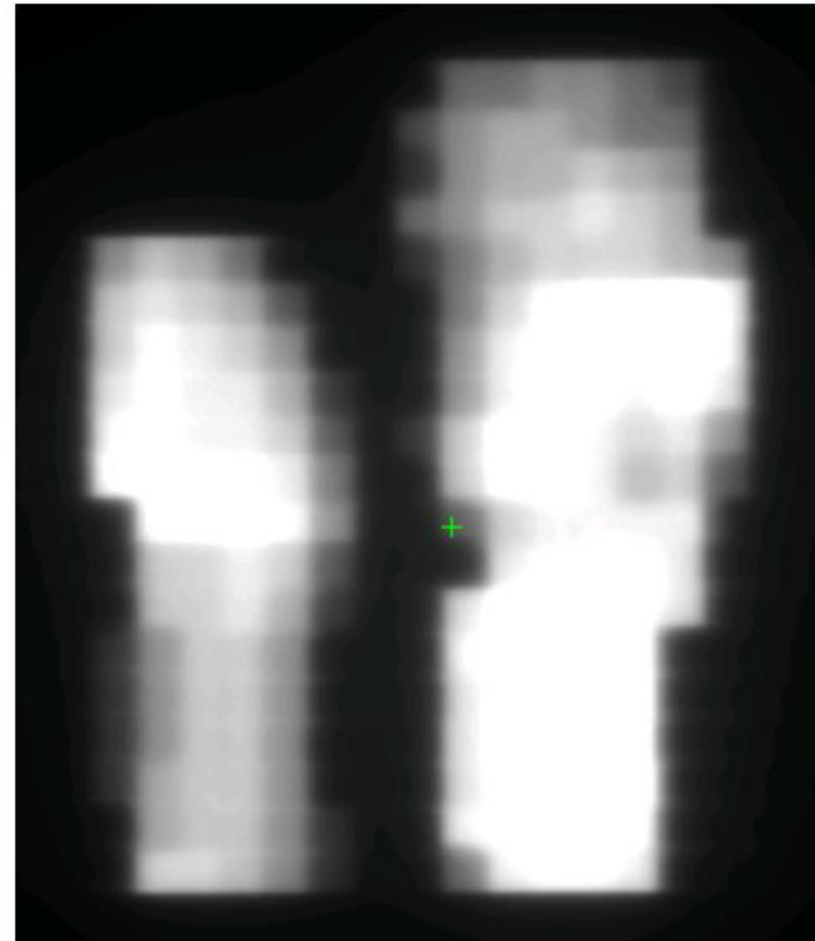
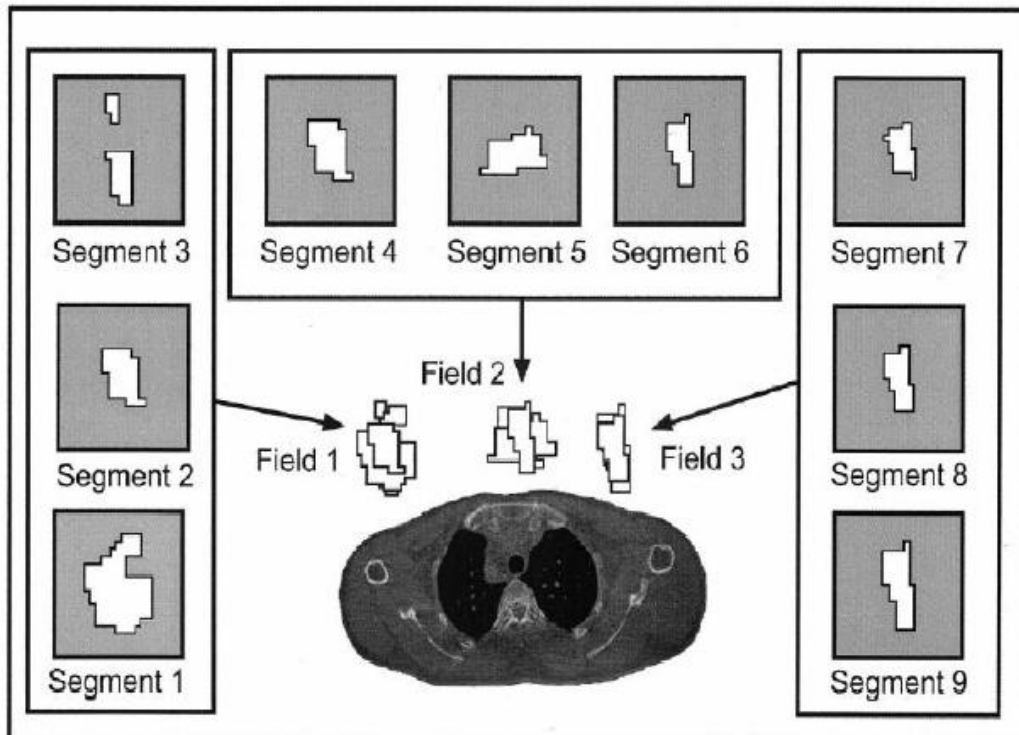
Multi Leaf Collimators (MLC)

Dose conformation obtained using Multileaf Collimators with sets of mobile lamellae in W mounted externally on the LINAC head



Example: IMRT irradiation in step and shoot modality, the total dose is released as a sum of nine segments, each corresponding to a particular arrangement of the MLC lamellas (left). Beam is off during their movement.

Total dose is obtained as the sum of the dose released by each segment (right).



VMAT (*Volumetric Modulated Arc Therapy*)

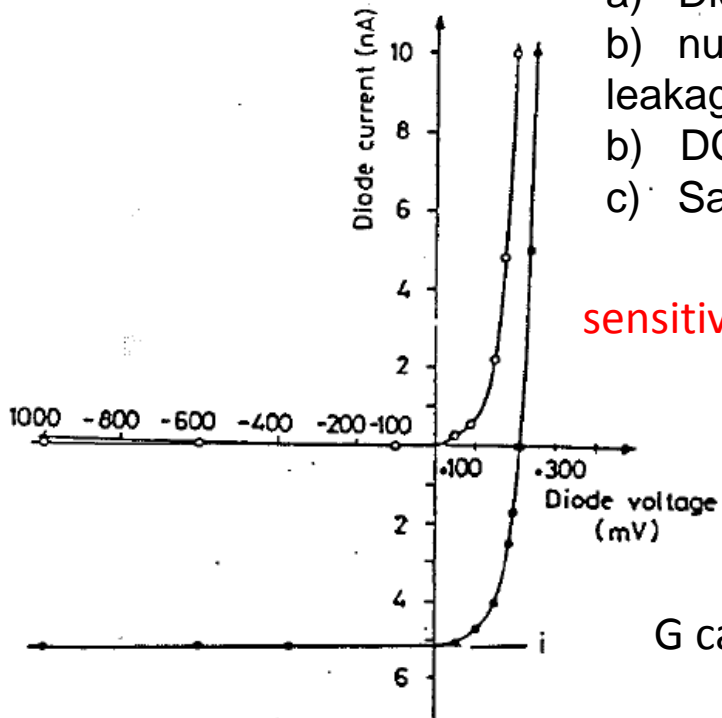


- ❑ Able to focus more accurately at tumor tissues, ensuring greater preservation of healthy ones.
- ❑ Modulating not only the amplitude and velocity of the MLC, but also **rotation speed of the Gantry and Linac dose-rate**.
- ❑ **continuous rotation of the accelerator head during irradiation for maximum focusing** of radiation on tumor tissues, which are thus affected by all possible angles.
- ❑ **significantly reducing duration of treatments** compared to IMRT: about 5-7 minutes compared to traditional times which are around 20 minutes per session.
- ❑ **useful when treatment focus must be maximum to preserve nearby organs:** tumors of the head / neck, as larynx, pharynx and oral cavity; tumors of the pelvis, as prostate and rectum; tumors of the lung and breast.

Working principle of a on-line dosimeter



- a) Diode / resistor
- b) null bias or low bias (to minimize leakage current and polarization effects).
- b) DC coupling.
- c) Sampling time and reset fixed by digital electronics ($t \geq 10\text{ms}$).



sensitivity $S = \frac{Q}{D \text{ Volume}} = \frac{qG}{R}$

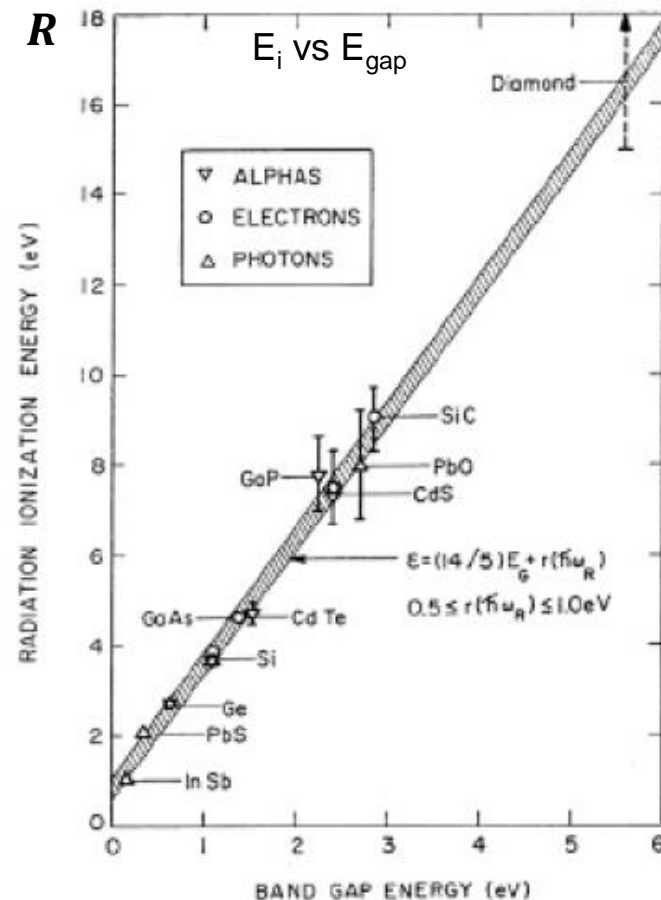
R,: dose rate;
 Q: released charge;
 D: delivered dose;
 q: elementary charge

G carrier generation rate:

$$G = \frac{R\rho}{E_i}$$

ρ : density;
 E_i : mean ionization energy.

$\rightarrow S = \frac{q\rho}{E_i}$



	IC(AIR)	SILICON	DIAMOND	CsPbBr3
ρ [g/cm ³]	1.29×10^{-3}	2.33	3.52	4.55
E_i [eV]	34.00	3.60	16.20	5.30
Sensitivity [nC/Gymm ³]	0.038	647.22	217.28	860

Dosimetry Challenges



Highly accurate imaging and dose verifications systems must match with increased accuracy of the irradiation techniques .

- **Response independent of energy** - often Charged Particle Equilibrium (CPE) lacks (a phenomenon associated with the range of secondary particles and hence dependent on the beam energy, composition and density of the medium);
- **small volume and high sensitivity** - to get enough spatial resolution;
- **response independent of dose rate**, continuously changing during VMAT;
- **Real time invivo detectors** - european community require dose delivery to be verified experimentally **directly during irradiation** (Article 56 of COUNCIL-DIRECTIVE-2013/59/EURATOM).

State-of-art commercial dosimetric devices used in clinical radiotherapy



	IC (AIR)	SILICON	DIAMOND
ρ [g/cm³]	1.29x10⁻³	2.33	3.52
E_i [eV]	34.00	3.60	16.20
S [nC/Gymm³]	0.038	647.22	217.28
Area [mm²]	25.00	0.64	3.80
thickness [mm]	5.00	0.03	0.001
volume [mm³]	125	0.019	0.0038
Array	OCTAVIUS PTW	MAPCHECK SunNuclear	-
Detector	729 PTW	SunPoint® Diode Detector	microDiamond type 60019 PTW
Reference	APL Mater. 7, 051101 (2019); doi: 10.1063/1.5083810		



OCTAVIUS® Systems

Turnkey Solutions for Patient and Machine QA



Products & Solutions > Radiation Therapy > VMAT QA, IMRT QA, OCTAVIUS, DIAMOND > OCTAVIUS 729 > Specifications

▼ PRODUCTS & SOLUTIONS

- ▶ Radiation Therapy
- ▶ Diagnostic Radiology
- ▶ Health Physics

▶ SERVICES & SUPPORT

▶ LITERATURE

▶ NEWS & EVENTS

▶ ABOUT PTW

▶ REFERENCE SITES

▶ DOWNLOAD CENTER

▶ ONLINE BROCHURES

▶ THE DOSIMETRY SCHOOL

▶ CONTACT US

▶ LINKS

▶ FEEDBACK

advanced search

OCTAVIUS 729

Specifications

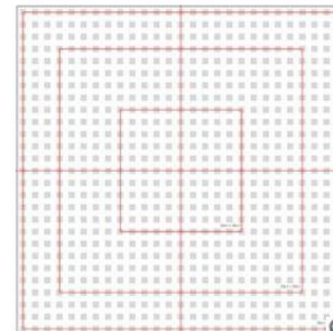
Learn more

OCTAVIUS Detector 729

- ▶ **Detector type:** Plane-parallel vented ionization chambers
- ▶ **Detector design:** cubic
- ▶ **Number of detectors:** 729
- ▶ **Detector size:** 0.5 cm x 0.5 cm x 0.5 cm (0.125 cm³)
- ▶ **Detector spacing:** 10 mm center-to-center, 5 mm edge-to-edge
- ▶ **Max. field size:** 27 cm x 27 cm
- ▶ **Reproducibility:** $\leq \pm 0.5\%$
- ▶ **Dead time:** zero
- ▶ **Repetition rate:** 200 ms
- ▶ **Measured quantities:** absorbed dose to water (Gy), absorbed dose rate to water (Gy/min)
- ▶ **Resolution:** 0.1 mGy or 0.1 mGy/min
- ▶ **Measurement range:** (0.5 ... 48 Gy/min)
- ▶ **Reference point:** 7.5 mm below the surface of the array
- ▶ **Housing material:** GRP
- ▶ **Dimensions:** 30 cm x 42 cm x 2.2 cm (W x D x H)
- ▶ **Weight:** 5.7 kg
- ▶ **Power supply:** (100 ... 240) VAC; (50 ... 60) Hz
- ▶ **PC connection:** Ethernet, RS232
- ▶ **Part No.:** L981378



OCTAVIUS® 729 - 2D ionization chamber array for patient and machine QA with OCTAVIUS 2Di/4D



729 cubic ionization chambers uniformly arranged on 27 cm x 27 cm

ArcCHECK® & 3DVH®

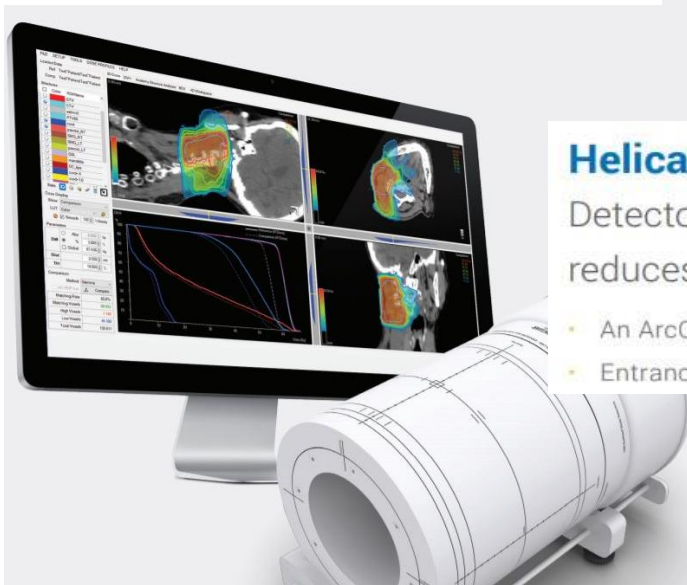
The Ultimate 4D Patient QA Solution



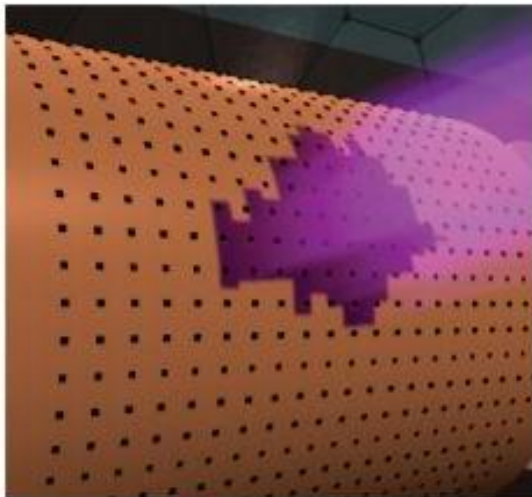
Helical Detector Grid

Detectors are arranged on a HeliGrid™ which increases the sampling rate and reduces BEV detector overlap and shadowing.

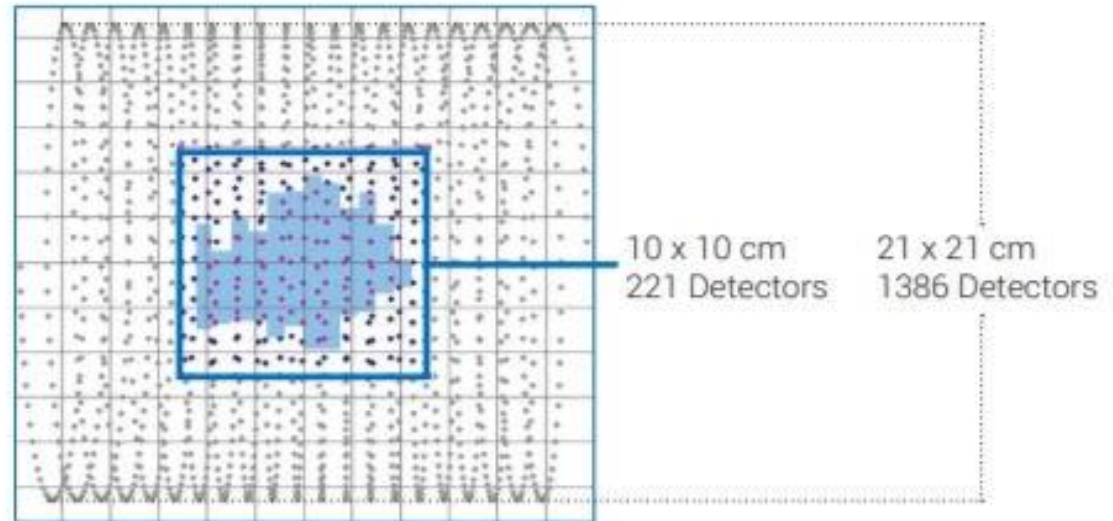
- An ArcCHECK 10 x 10 cm² area contains 221 detectors; equivalent to the detector density in a MapCHECK® 2
- Entrance and exit dose are measured, effectively doubling the detector density in the measurement field



Beam Delivery



ArcCHECK Detector



The Silicon Choice

Advantages:

- High sensitivity (18000 times higher than IC).
- Well developed manufacture technology.
- high spatial resolution.
- work in null bias mode (in-vivo).

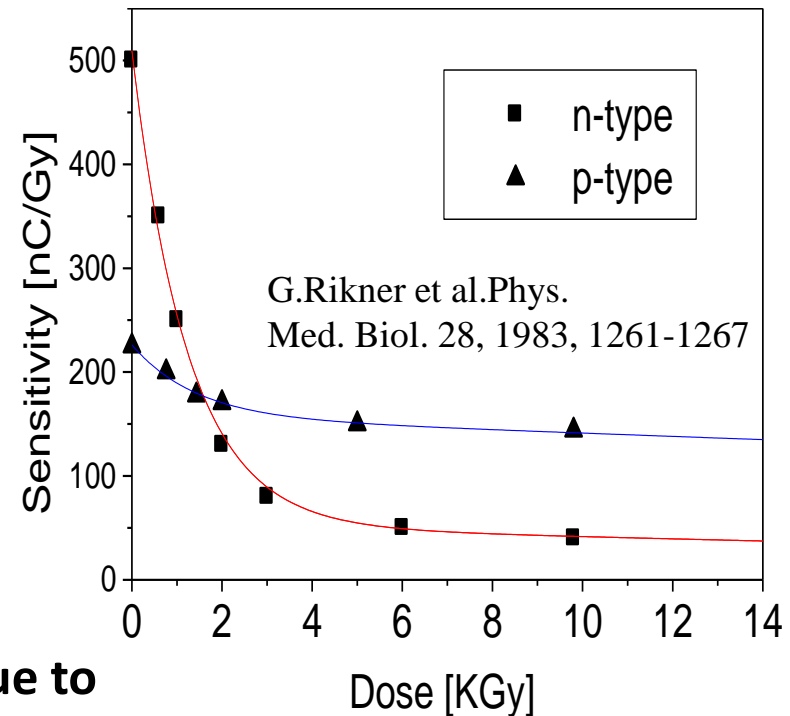
Drawbacks:

- Sensitivity decrease with accumulated dose due to increase of concentration of recombination centers (recalibrations needed).
- Dose rate dependency due to centers saturation at high dose rates.
- Energy dependence: Si not "water equivalent".

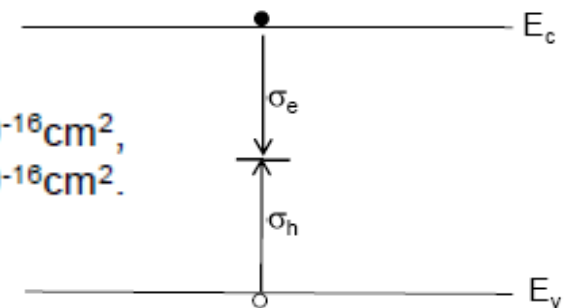
Radiation Resistant ?

p-type radiation harder material

hole capture more efficient -> Lifetime for minority carriers higher in case of electrons.



$$\sigma_e = 1.62 \times 10^{-16} \text{cm}^2,$$
$$\sigma_h = 8.66 \times 10^{-16} \text{cm}^2.$$



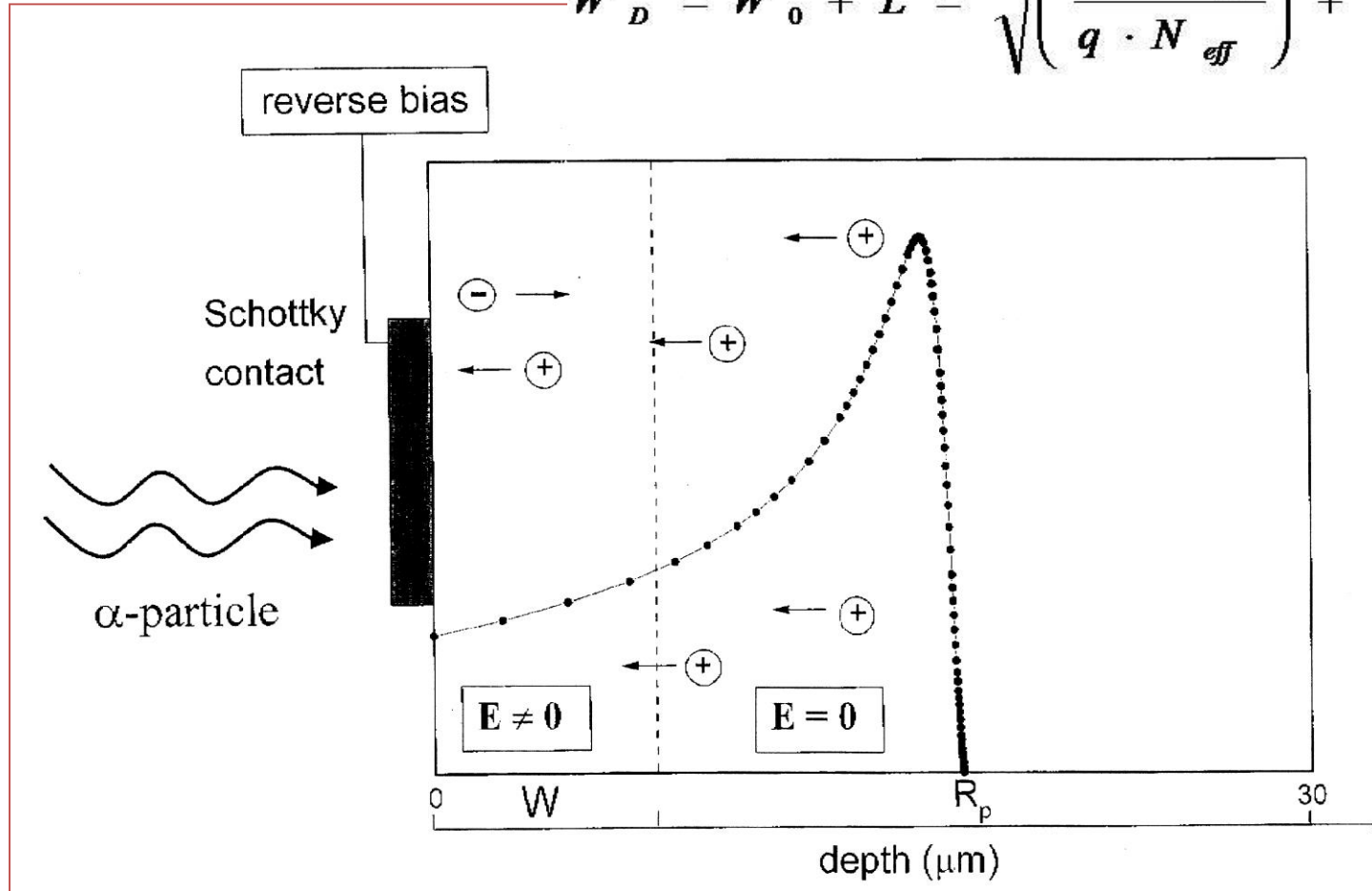
Dosimeter active region

W = depletion thickness

R_p = particle range

L = diffusion length

$$W_D = W_0 + L = \sqrt{\left(\frac{2 \epsilon \cdot V_{bi}}{q \cdot N_{eff}}\right)} + \sqrt{D_h \cdot \tau_h}$$

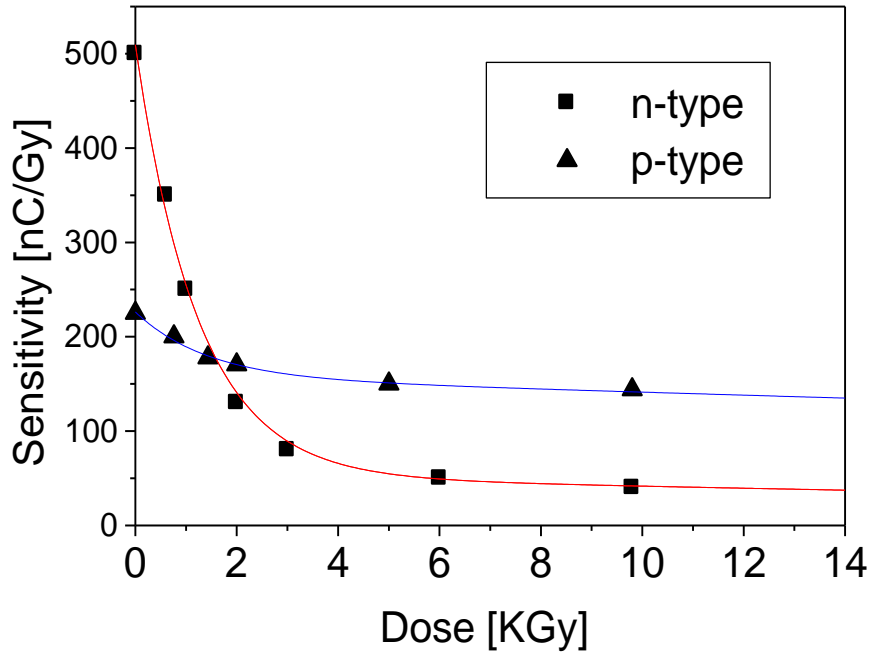


The neutral region contributes (diffusion of minority carriers into the depletion region) to the signal

Radiation damage in standard Si dosimeters (thickness 300um)

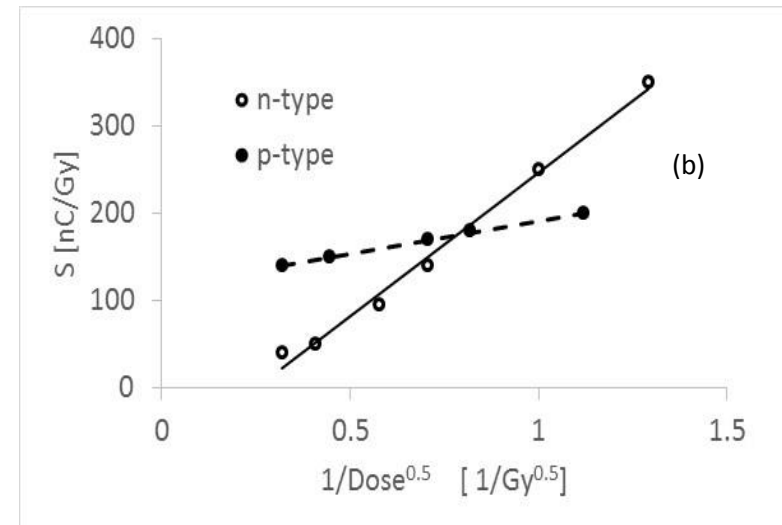
Sensitivity as a function of trap concentration in a Si dosimeter

$$S = \frac{q\rho_{Si}}{E_i} \sqrt{\frac{D_e}{\sigma_e v_e N_t}} \propto N_t^{-1/2}.$$



N_t linearly increasing with dose so:

$$S \propto \frac{1}{\sqrt{Dose}}$$

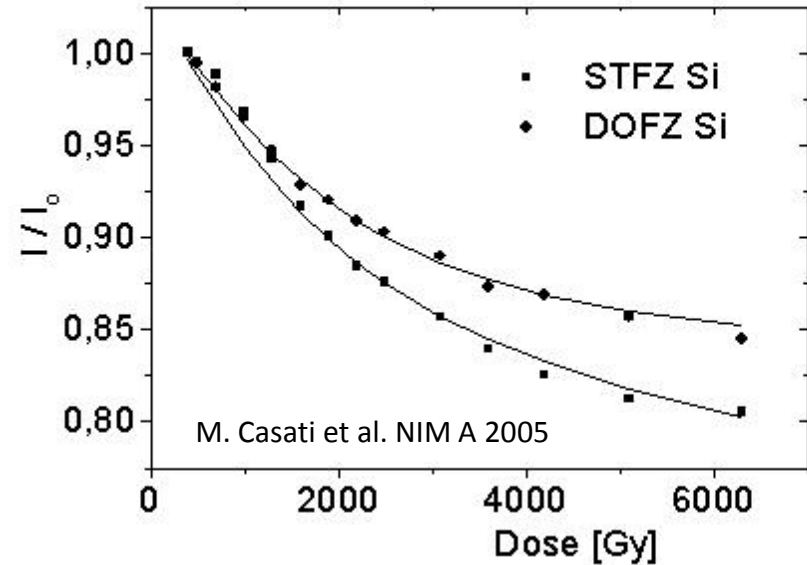


M. Bruzzi, NIMA 809, 2016 Novel Silicon Devices for Radiation Therapy Monitoring, 105-112

Pre-irradiation (≈ 10 KGy) to reduce the dependence of the signal on the dose.

Material engineering concepts have been applied also to Silicon dosimeters for radiotherapy

Improved radiation hardness of DOFZ Si



Decrease in sensitivity with the accumulated dose due to the generation of a dominant trap acting as lifetime killer.

$$1/\tau - 1/\tau_0 = \sigma v_{th} N_t$$

$$N_t = a \phi; \quad a = \text{trap generation rate}$$

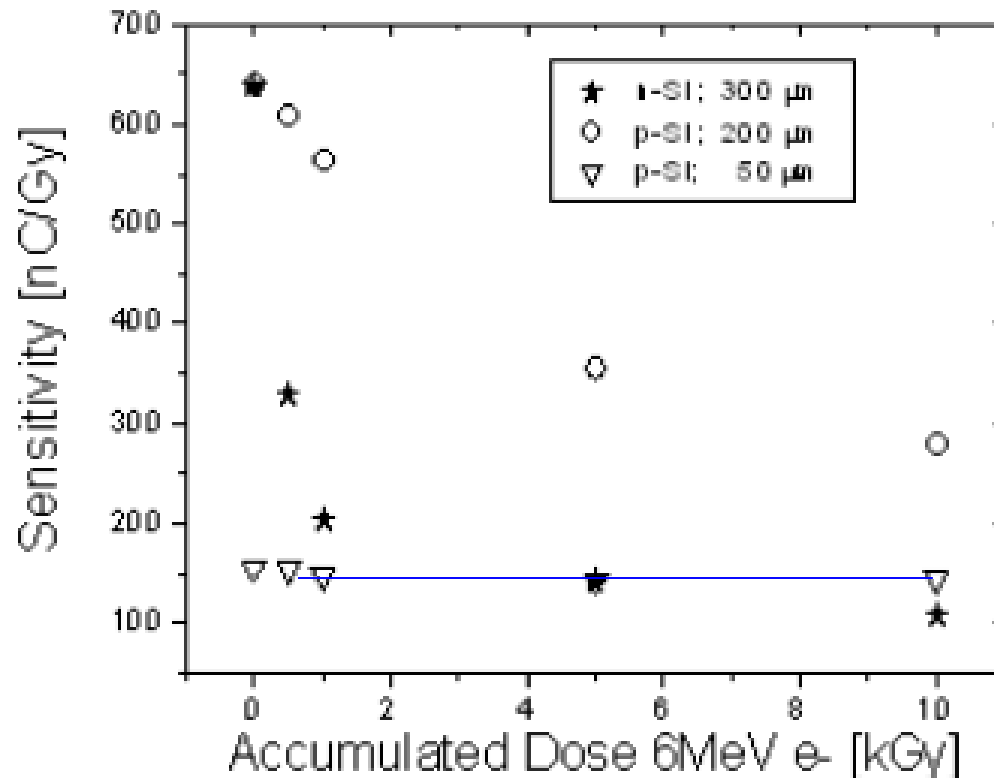
σ capture cross section ; v_{th} carrier thermal velocity. N_t trap concentration.

$a_{DOFZ} < a_{SFZ} \Rightarrow$ increased radiation hardness of the device to radiotherapeutic beams.

$$a_{DOFZ} = 5.0 \times 10^7 \text{ cm}^{-3} \text{ Gy}^{-1}, \quad a_{SFZ} = 8.1 \times 10^7 \text{ cm}^{-3} \text{ Gy}^{-1}$$

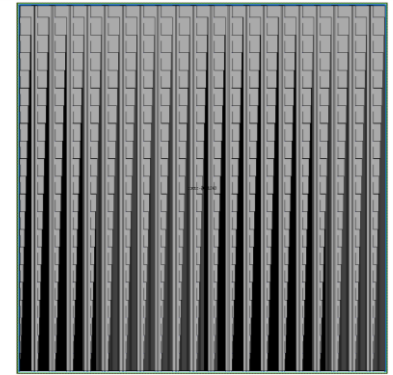
Our recipe: epitaxial p-type Si on MCz substrates to limit active thickness

Active region is limited in any direction to a value shorter than L_n at the highest dose of interest. Epitaxial Layer is used to limit active depth, guard-ring to limit active area.



M. Bruzzi et al., "Epitaxial silicon devices for dosimetry applications," Appl. Phys. Lett., vol. 90 (2007) 172109 1-3.

Si bidimensional dosimeter



Matrix: 21x21pixels

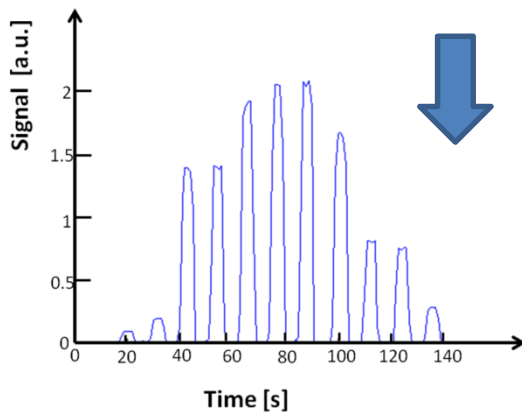
Pixel: 2x2mm Pitch: 3mm

Detector size: 6.3x6.3cm²

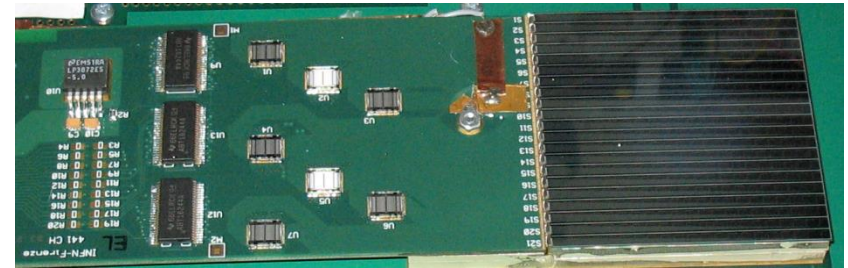
Covered area 20x20 cm²
~4k channels

C.Talamonti, M.Bruzzi et al. 2011 Nucl. Instr. Meth A, vol. 658, p. 84-89.

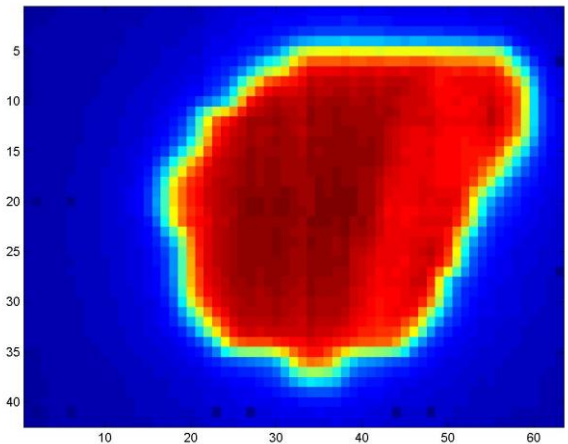
Measured time structure of dose segments



Large area IMRT covered by mosaic composition and/or shifting modules along x-y axes.



Dose map of an IMRT field for prostate cancer as measured by the Epi-Si 2D silicon dosimeter.



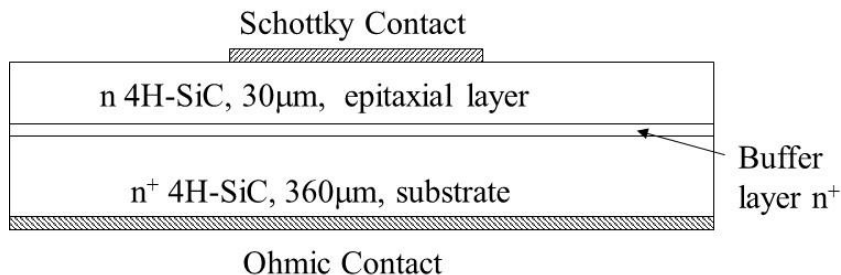
United States Patent
 Bruzzi et al.

(10) Patent No.: M. Bruzzi, INFN Firenze Cds 2 Marzo 2020
 (45) Date of Patent:

US 8,563,936 B2
 Oct. 22, 2013

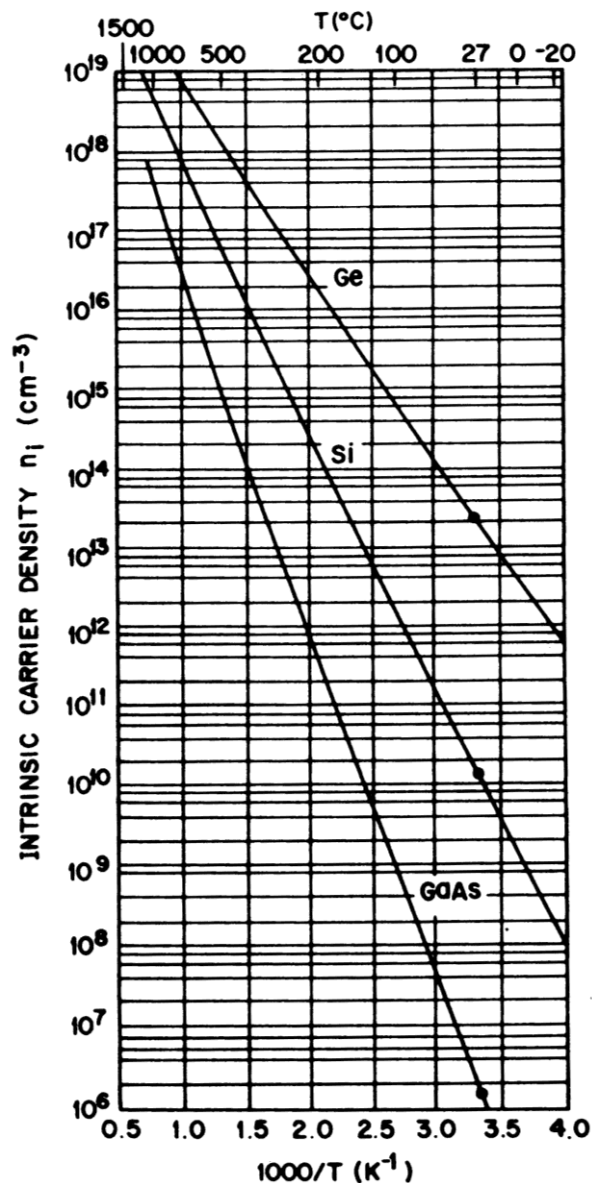
The SiC choice

- ☺ Low Leakage Current
- Working without applying bias
- Very low active volume
- Fast Response
- More tissue equivalent than Si
- ♠ Radiation resistance ?



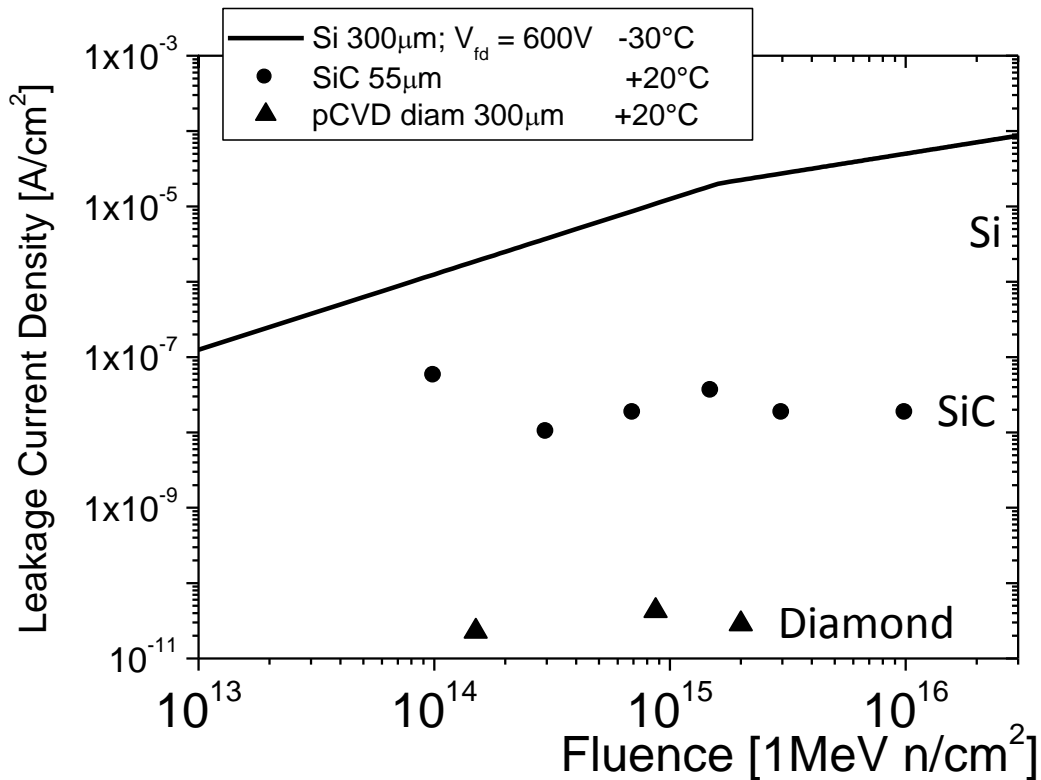
materiale	Z
aria	7.78
acqua	7.51
muscolo	7.64
grasso	6.46
ossa	12.31
carbonio	6
silicio	14
SiC	~10

High bandgap semiconductors: generation always negligible → intrinsically radiation hard



$$J_{gen} \propto \frac{n_i}{\tau_g} W \quad n_i \propto T^{\frac{3}{2}} e^{-\frac{\epsilon_g(T)}{2K_B T}}$$

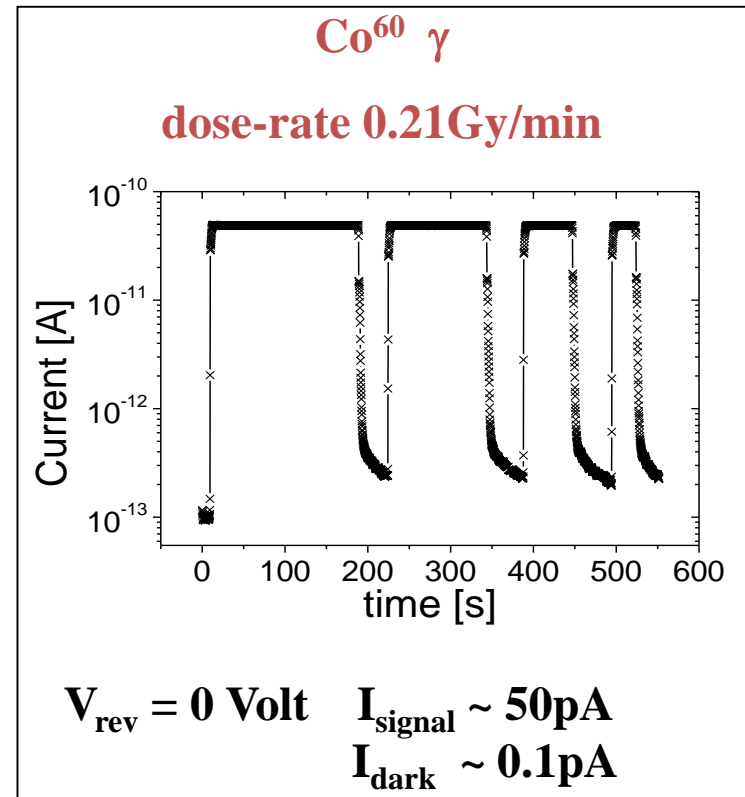
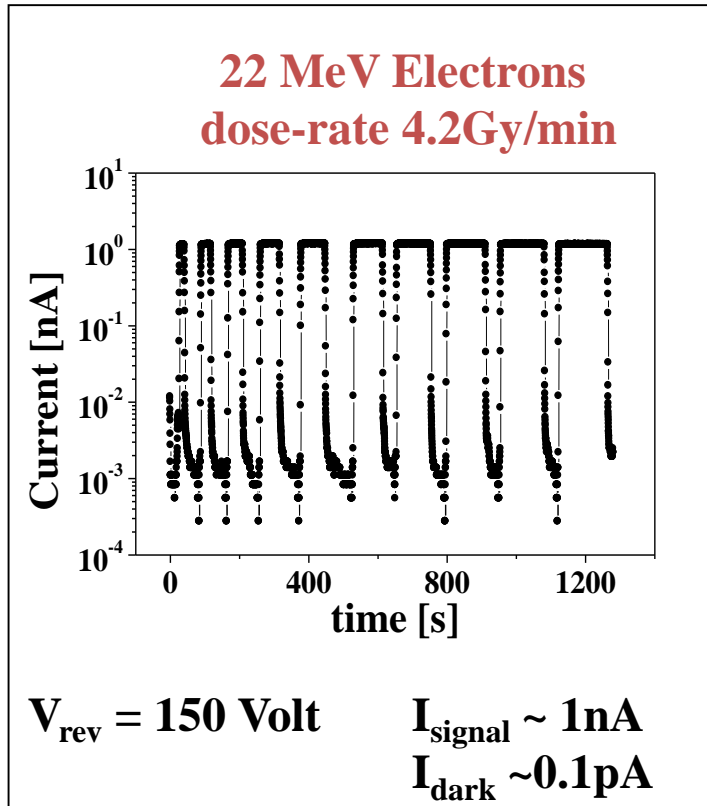
$T = -30^{\circ}\text{C}; V = 600\text{V}, W = 300\mu\text{m}$



M. Bruzzi ;H. Sadrozinski ; A.Seiden NIM A 579 2 754 (2007)

Dosimetric Characterisation

Stable signal - high S/N ratio - no priming effects

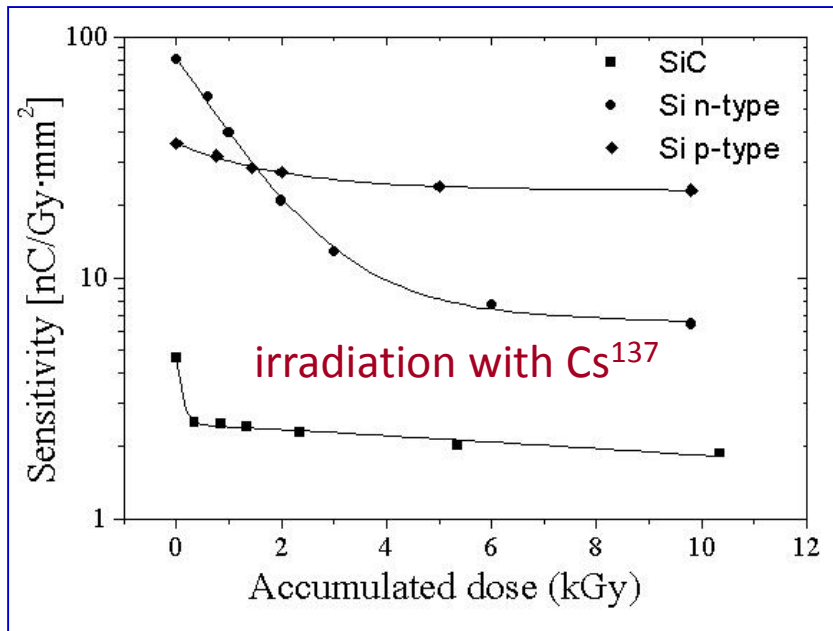


M. Bruzzi, F. Nava, S. Pini, S. Russo, App. Surf. Sci, 184 (2001) 425-430

Comparison between Epitaxial SiC and standard dosimeters

Device	bias [V]	Vol. [mm ³]	S [nC/Gy]	S per unit volume [nC/(Gy·mm ³)]
Standard Farmer Ionisation chamber	300	600	21.5	0.036
Miniature Farmer Ionisation chamber	300	50	1.38	0.028
Scanditronix GR-p BS Silicon	0	0.295	140	474
Scanditronix SFD stereotactic Silicon	0	0.017	6	353
Epitaxial SiC diode	0	0.0415	14.1	340

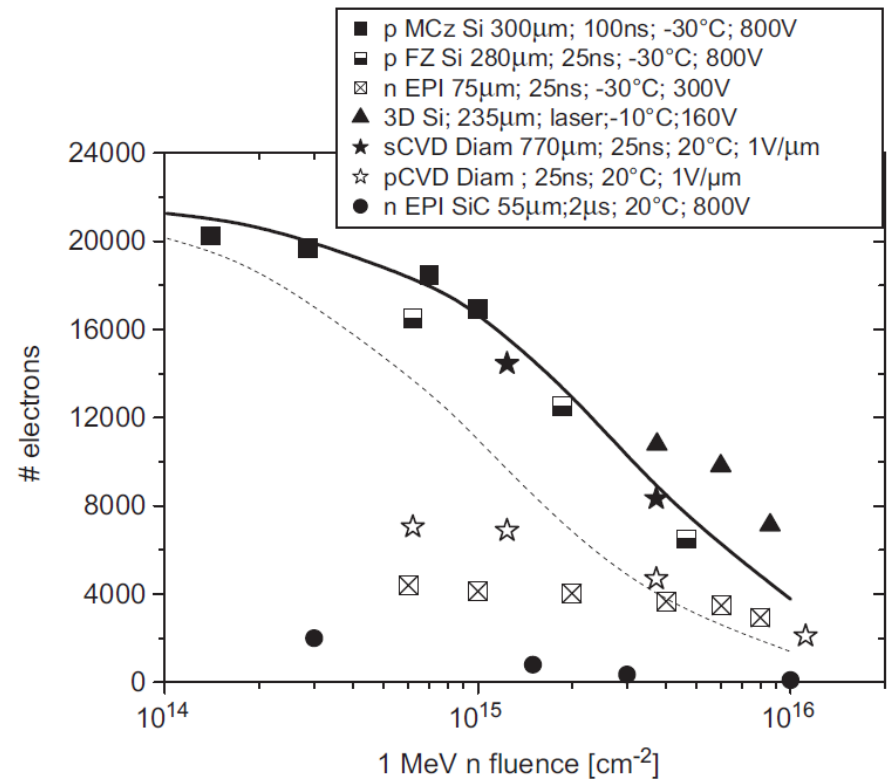
Problem: SiC is not defect tolerant



M. Bruzzi, F. Nava, S. Pini, S. Russo,
App. Surf. Sci, 184 (2001) 425-430

Worse sensitivity vs. Accumulated Dose than Si

Worse cce vs. fluence than Si

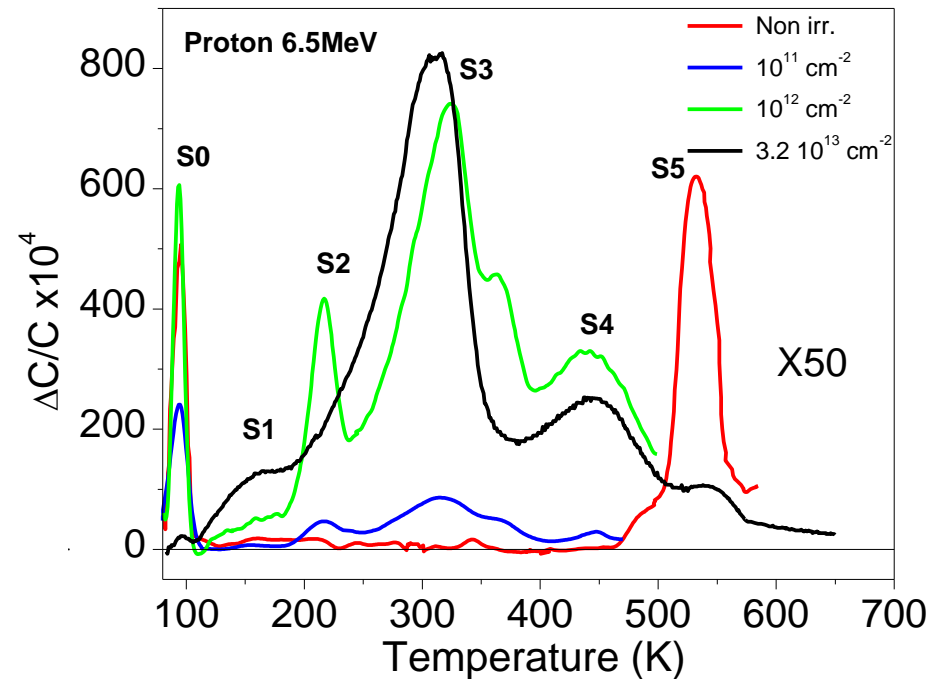


Microscopic radiation damage is responsible of the reduced charge collection of SiC with respect to Si and Diamond

- ◆ n epilayer $7\mu\text{m}$
- ◆ $N_{\text{eff}} \sim 7 \times 10^{15} \text{cm}^{-3}$
- ◆ Schottky Barriers Ti or Ni
- ◆ Ohmic contacts Ti/Ni/Ag
- ◆ Deep levels by C-DLTS
- ◆ 6.5MeV p up to $6.4 \times 10^{13} \text{cm}^{-2}$

Six traps detected after irradiation

- ◆ $E = 0.18 - 1.22 \text{eV}$
- ◆ $\sigma = 10^{-13} - 10^{-18} \text{cm}^{-2}$
- ◆ $N_t = 10^{11} - 5 \times 10^{14} \text{cm}^{-3}$



Data from A. Castaldini, A. Cavallini et al.

The Diamond Choice



- 😊 ■ it is almost water equivalent
 - it doesn't perturb the radiation field → small fields
 - the energy is absorbed as in the water → no correction factors
- high radiation hardness → long term stability
- high density → high sensitivity → small dimensions
- non toxic
- it can be used as TL dosimeter (off-line) or for on-line applications

- ♠ ■ high defect density - priming effects – instability of the signal
- high voltage required
- high production costs

Nearly as good as water.

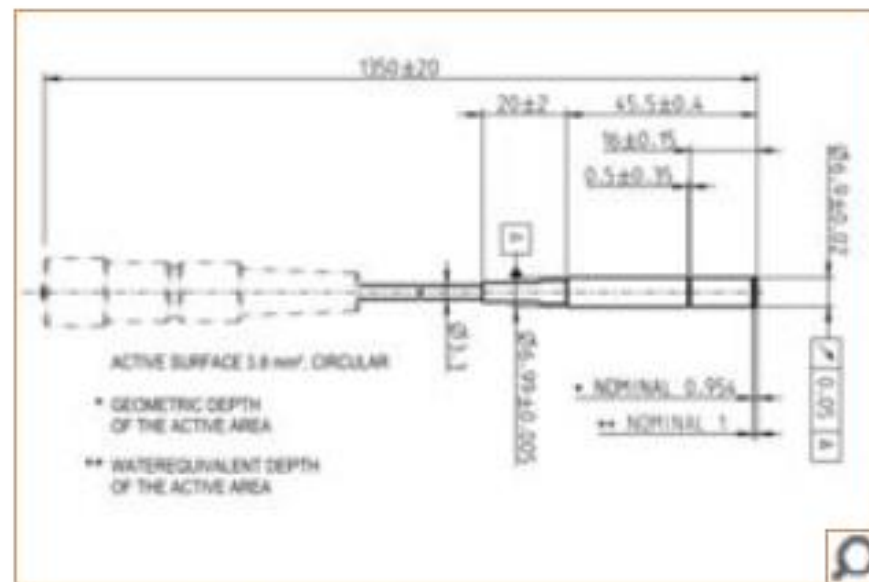
microDiamond

Key Features

- ▶ Nearly water equivalent for all beam energies
- ▶ Very small sensitive volume (0.004 mm^3) - perfect choice for small field dosimetry
- ▶ Suitable for all field sizes up to $40 \text{ cm} \times 40 \text{ cm}$
- ▶ Precise, accurate measurements in photon, electron and proton fields
- ▶ Excellent radiation hardness, minimal energy, temperature and directional dependence
- ▶ No high voltage required. Suitable for all connecting systems (BNT, TNC, M)

▶ Type No.	60019
▶ Design:	waterproof, disk-shaped, sensitive volume perpendicular to detector axis
▶ Measuring quantity:	absorbed dose to water
▶ Nominal sensitive volume:	0.004 mm^3 , radius 1.1 mm , thickness $1 \mu\text{m}$
▶ Reference point:	on detector axis, 1 mm from detector tip, marked by ring
▶ Nominal response:	1 nC/Gy
▶ Detector bias:	0 V
▶ Radiation quality:	$100 \text{ keV} \dots 25 \text{ MV}$ photons $(6 \dots 25) \text{ MeV}$ electrons $(70 \dots 230) \text{ MeV}$ protons
▶ Field size:	$(1 \times 1) \text{ cm}^2 \dots (40 \times 40) \text{ cm}^2$
▶ Connectors:	BNT, TNC or M

microDiamond Synthetic Diamond Detector

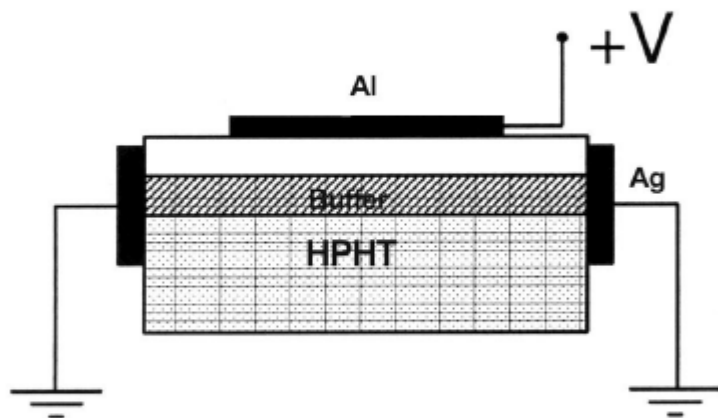


microDiamond Detector Design

Single Crystal Diamond Dosimeter

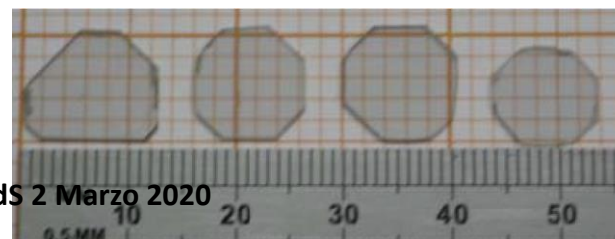
device manufactured by Università di Roma Tor Vergata

Schottky barrier $V_{rev} = 0$



- HPHT p+ boron doped substrate - 300 μm thick
- 35 μm thick p+ buffer layer (CVD)
- Active epilayer 17 μm thick
- Al 100 nm ϕ 2mm upper electrode
- Buffer layer contacted at the periphery with Ag paste

Problem : No large area array available



The Polycrystalline diamond Choice



- **it is almost water equivalent**



it doesn't perturb the radiation field → small fields

the energy is absorbed as in the water → no correction factors

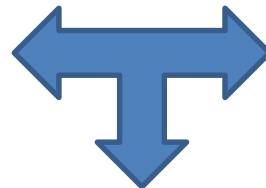
- **high radiation hardness** → long term stability

- high density → high sensitivity → small dimensions

- non toxic

Natural diamond

- very high production costs, difficult to select stones with proper dosimetric response ♠



Polycrystalline CVD diamond

Single crystal CVD
(Chemically Vapour
Deposited) diamond

- grown on HPHT diamond, not available in large areas ♠



ability to produce large area wafers of 3-5"

- persistent currents due to trapping → slow dynamics ♠

Neutron irradiation in pCVD diamond beneficial as removes dominant defect and increase recombination centres, bringing to faster dynamics

Measurements of pCVD diamond photoresponse under different cycles of X-ray irradiations – deactivation of the peak at 1eV probably responsible of the current instability.

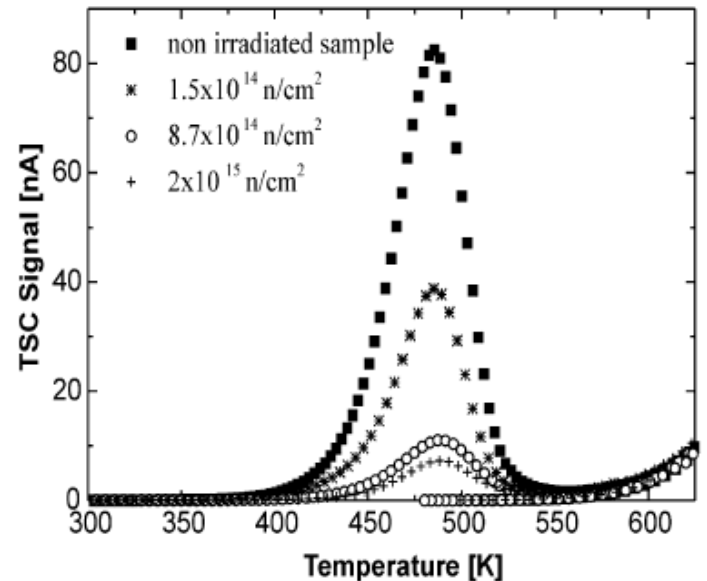
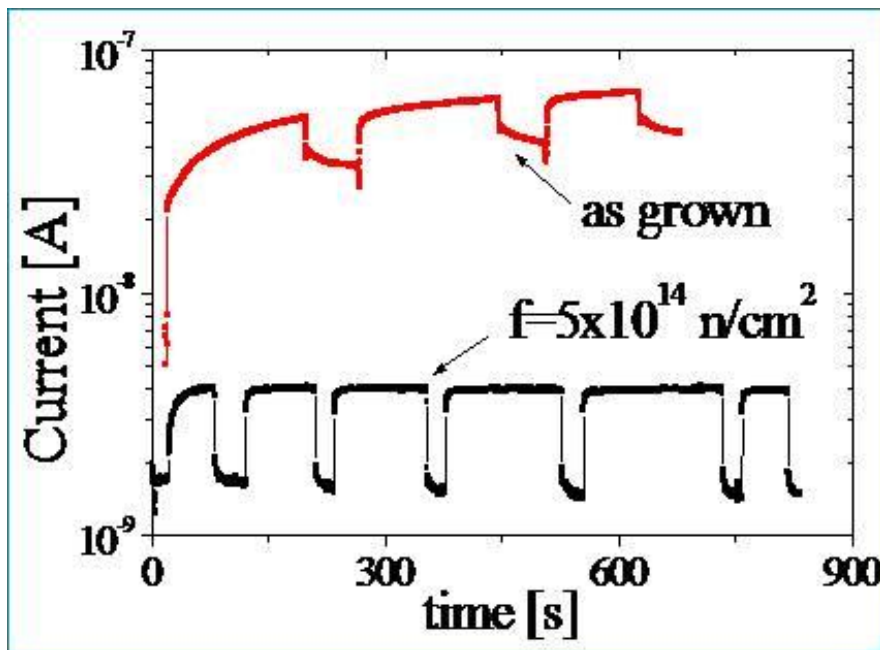


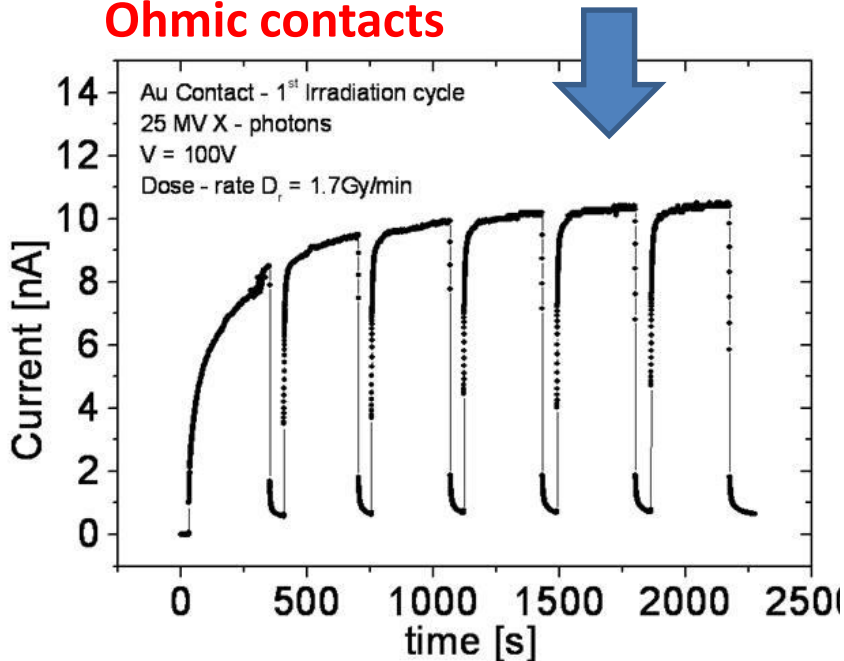
Fig. 1. TSC signal vs. temperature for non-irradiated and irradiated samples, after filling with UV xenon lamp for 20 min. The samples are biased with 100 V. The heating rate is 0.15 K/s. The neutron fluences are indicated in the legend.

M. Bruzzi et al., Appl. Phys. Lett, (2002)

Problem in polycrystalline diamond: priming and instability effects due to defects at grain boundaries



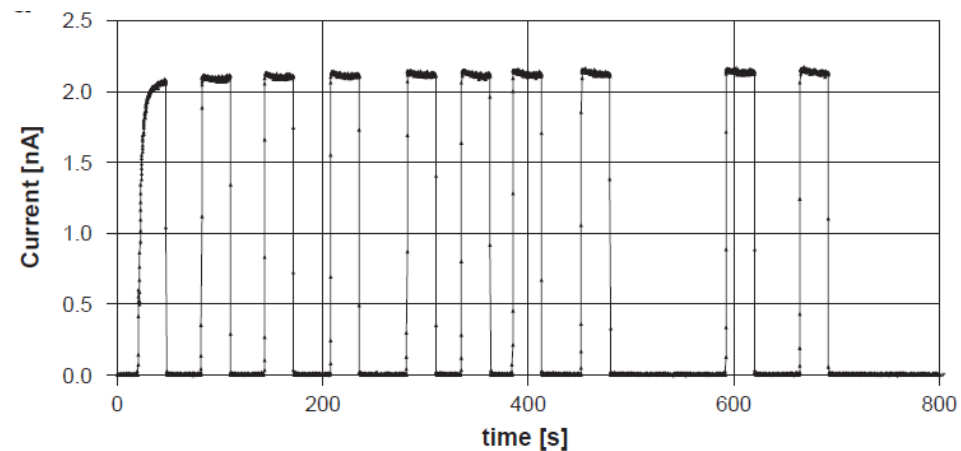
High voltage application
Ohmic contacts



Current response of the unirradiated sample (Au contact) showing the priming effect during the first 6 successive irradiations.

Our Solution to get STABLE SIGNAL

- back to back schottky barriers
- low/null bias



Diamond & Related Materials 20 (2011) 84–92

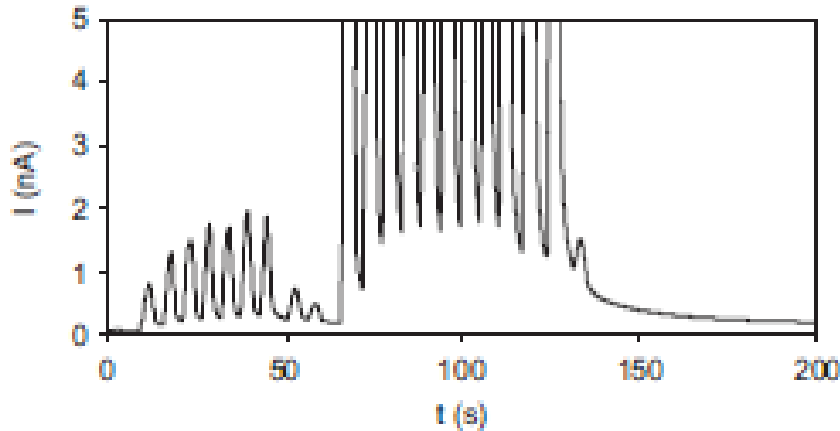
Zero-bias operation of polycrystalline chemically vapour deposited diamond films for Intensity Modulated Radiation Therapy

M. Bruzzi ^{a,*}, C. De Angelis ^b, M. Scaringella ^a, C. Talamonti ^c, D. Viscomi ^b, M. Bucciolini ^c

M. Bruzzi, INFN Firenze CdS 2 Marzo 2020

Priming and instability effects due to trapping and polarization in pCVD are dominant at high voltage with ohmic contacts and high electric field applied.

Slow dynamics due to persistent currents in pCVD in conventional beam and in IMRT modality



C. De Angelis et al. / Nuclear Instruments and Methods in Physics Research A 583 (2007) 195–203

Polarization is negligible at low/zero bias operation when using Schottky contacts.

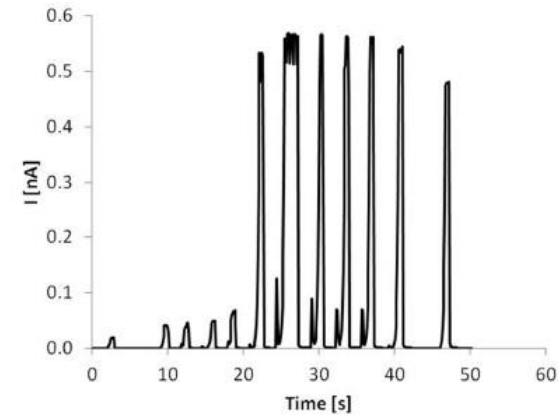


Fig.5 Time structure of the IMRT segments as measured by one of the pCVD diamond pixels under an IMRT prostate cancer treatment.

M. Scaringella et al. / Nuclear Instruments and Methods in Physics Research, A, 796, 2015, 89-92

M. Bruzzi et al. / Diamond & Related Materials 20 (2011) 84–92

polycrystalline diamond segmented dosimeter prototype made in Florence

- Material

- Up to three polycrystalline diamond films
- 2.5x2.5cm² active area each, 300μm thick;
- Premium Detector Grade Element Six, UK

- Contacts

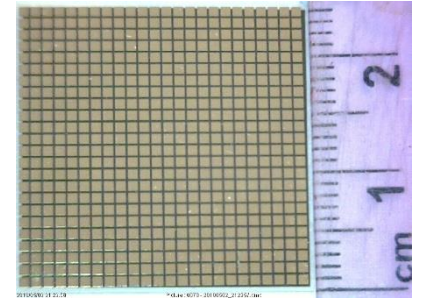
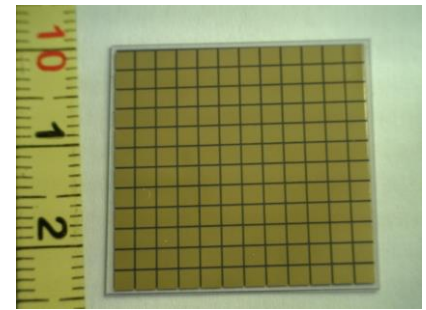
- Schottky Barriers produced @ University of Florence
- 12 x 12 matrix, pixel size: 1.8x1.8 mm² → 288 pixels in total

- Read Out Electronics

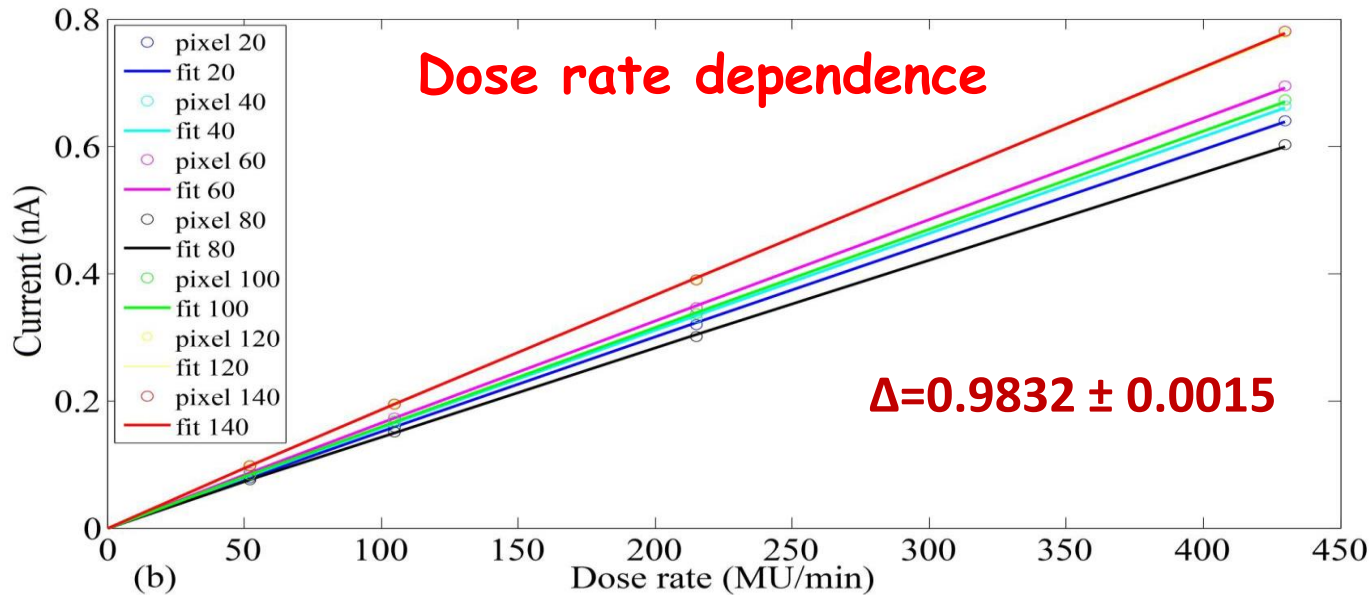
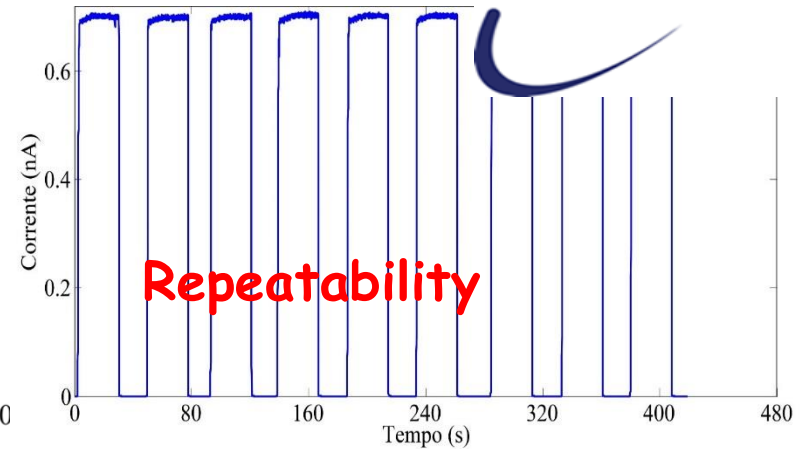
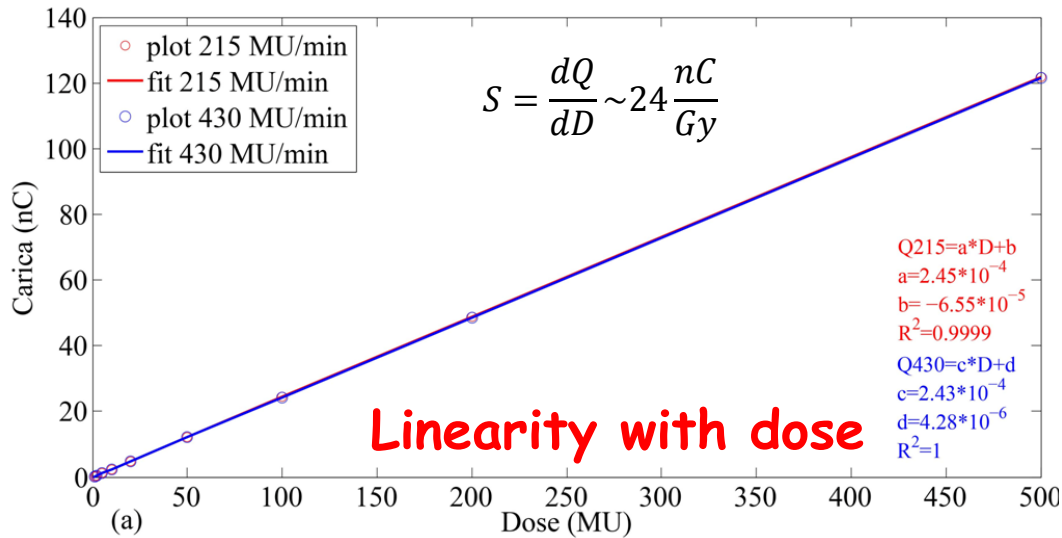
- four 64 channels 20 bit current-input analog to digital converter chips able of measuring currents from fAs to mAs; 160μs-1s integration time (50ms)
- custom printed circuit board;
- semi-rigid silver-polymer pin-contacts produced by us connecting each pixel of the 144 matrix connecting vias on PCB .

-Measurement

- Low voltage to get fast and reproducible signals;
- Device can be moved in x-y directions to cover a
- wider radiation field area.



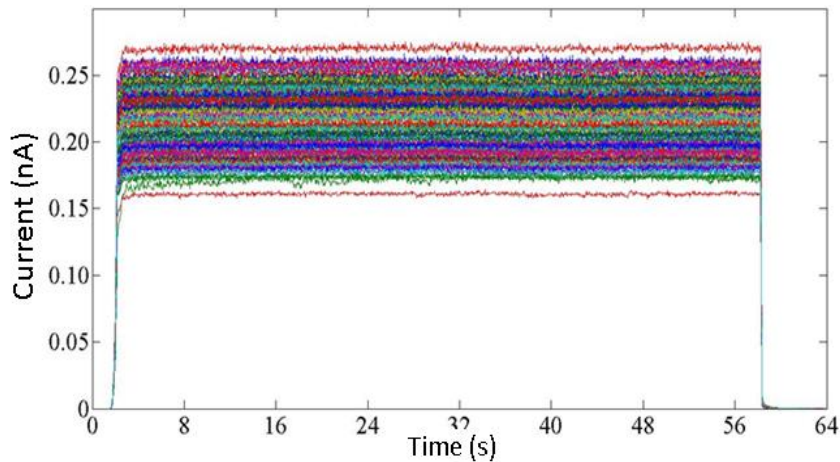
pCVD Diamond test under linac



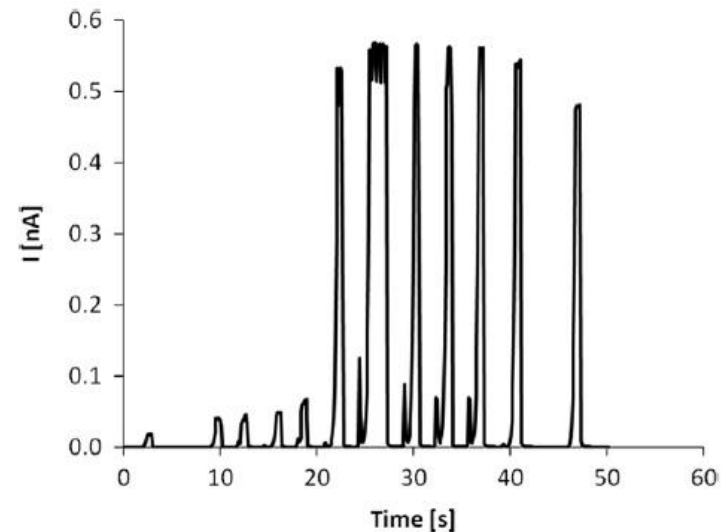
Performance under conventional and IMRT radiotherapy beam



Current response of all pixels in a conventional X-ray beam ($V_{app} = 1V$)
Dose-rate 50 Mu/min



Current response of one pixel under an IMRT beam in step and shoot modality



Bartoli et al. 2017 JINST 12 C03052

- ✓ negligible dark current → high S/N
- ✓ negligible polarization effects → stable response , fast dynamics

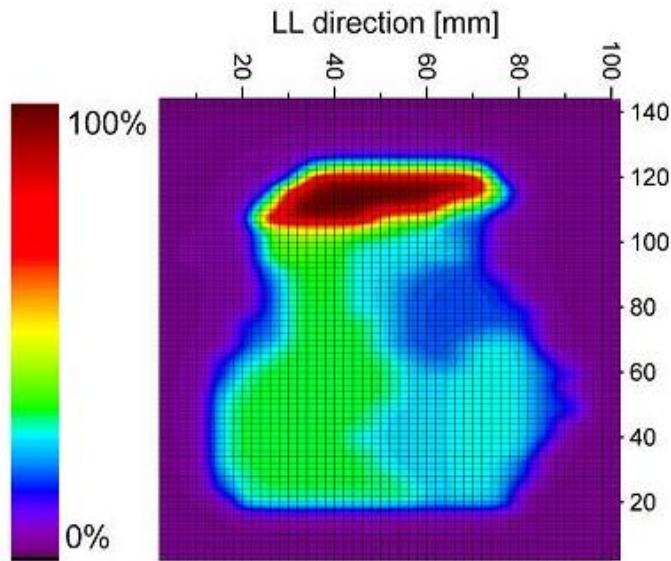
Fig. 5. Time structure of the IMRT segments as measured by one of the pCVD diamond pixels under an IMRT prostate cancer treatment.

M. Scaringella et al. ,

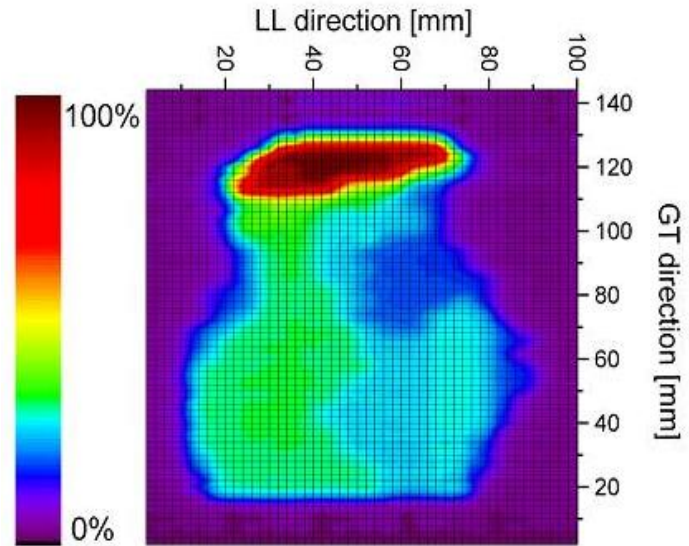
Nuclear Instruments and Methods in Physics Research A 796 (2015) 89–92

First IMRT map with Diamond Device

2.5x2.5cm² pCVD Diamond prototype
IMRT map 14x10cm²
measured by shifting the diamond dosimeter



IMRT breast cancer map **as measured by the pCVD Diamond .**



IMRT breast cancer map **as calculated by the TPS (treatment planning system)**

(GT = gantry target direction; LL = lateral-lateral direction) Grid spacing 3 mm.

M. Scaringella et al. / Nuclear Instruments and Methods in Physics Research A 796 (2015) 89–92

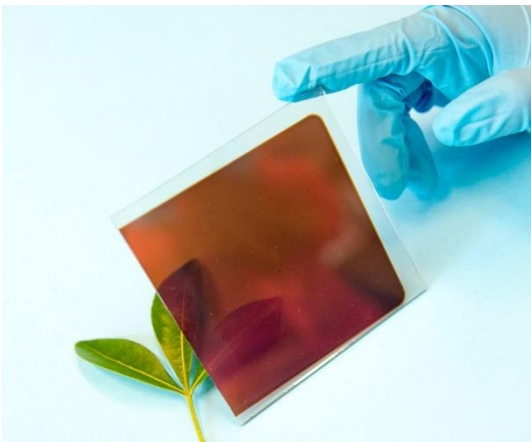
The Perovskite Choice

Perovskites are emerging materials for **large-area and flexible optoelectronic device systems**

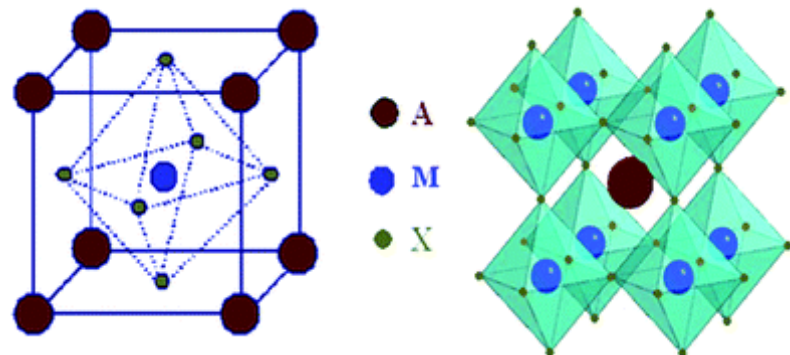
AMX_3 (**X = oxide, halide anion such as Cl, Br and I, M = metal cation**).

Organo-metallic halide perovskites **recently proposed for printable large area flexible X-ray detectors in medical imaging applications** (Nature 2017 550(7674): 87-91; Physics in Medicine, Vol. 5, 2018 20-23.).

All-inorganic perovskites, $CsPbX_3$ (X=Cl, Br, and I) attracting alternatives due to their improved chemical stability, they can be produced in form of single crystals, nano-crystals and micro-crystalline thin films.



A 15% perovskite solar cell made in University of Oxford



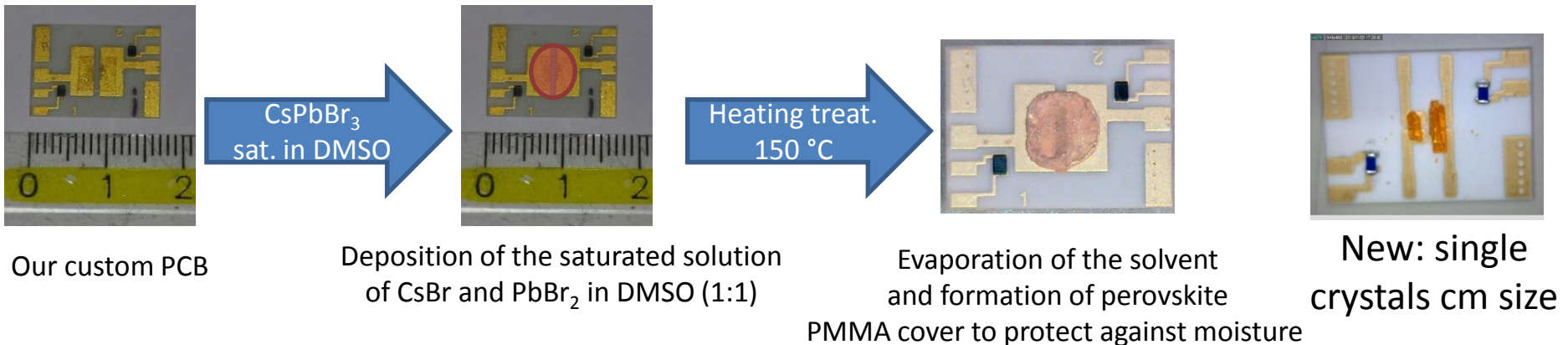
The CsPbBr₃ Choice



- More sensitive than silicon
- Easy deposition methods
- Potentially defect tolerant

	SILICON	CsPbBr ₃
E _g [eV]	1.12	2.30
ρ [g/cm ³]	2.33	4.55
E _i [eV]	3.60	5.30
S [nC/Gymm ³]	647.22	860

Sample preparation and characterization in Florence



- Possibility to deposit directly on any kind of substrates, even flexible
- Spin coating, magnetron sputtering, dropcast – polycrystalline and single crystals

Defect Tolerance of CsPbBr₃

Conventional semiconductors as GaAs, CdSe, InP, are defect intolerant as they are prone to mid-gap states very active as trap states.

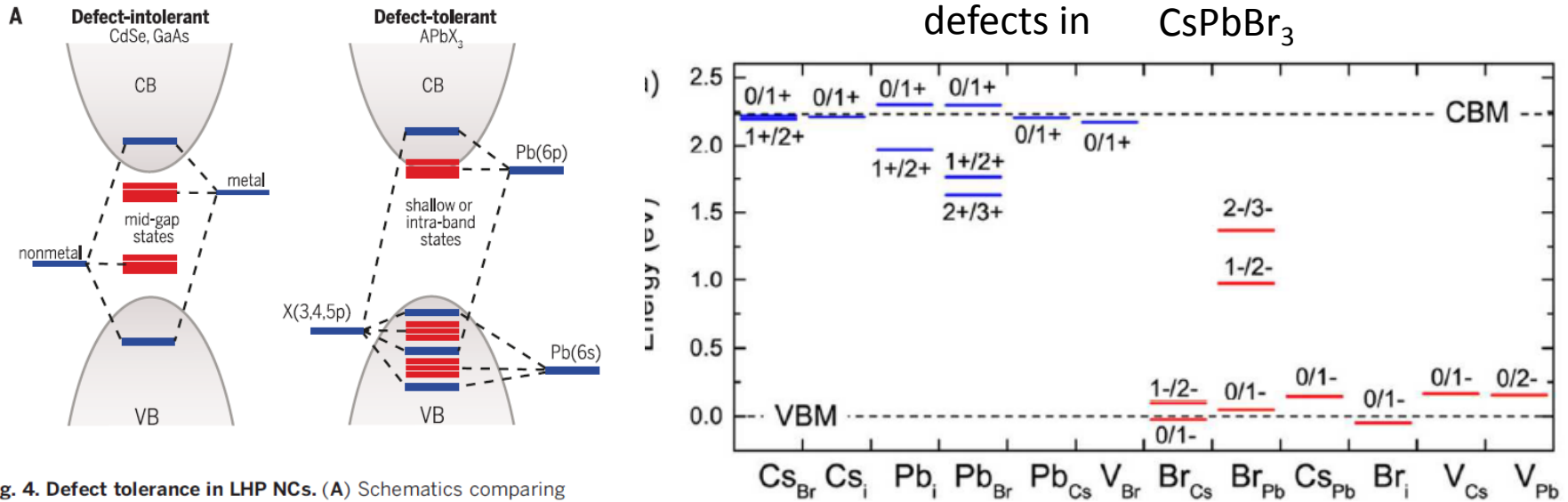


Fig. 4. Defect tolerance in LHP NCs. (A) Schematics comparing electronic structures that are defect-intolerant, such as for conventional semiconductors (for example, CdSe, GaAs, and InP), and defect-tolerant, such as for LHPs (27). Defects do not act as trap states in LHPs and are therefore benign toward their electronic and optical properties. [Adapted from (27)] (B) Electronic structure diagrams for CsPbBr₃ NCs at the DFT/PBE level of theory (26), where PBE is Perdew-Burke-Ernzerhof exchange-correlation functional. Each line

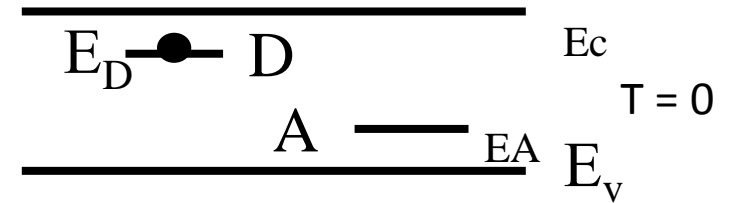
J. Kang, L.-W. Wang, *J. Phys. Chem. Lett.* **2017**, *8*, 489–493.

CsPbBr₃ potentially defect tolerant: mostly shallow and intermediate defect states.

Kovalenko *et al.*, *Science* **358**, 745–750 (2017)

Shallow levels: The hydrogen-like model

Donor (e.g. P in Si) is seen as a complex Si + H, an hydrogen atom is added at a site of the silicon lattice.



$$E_{Dn} = -\frac{e^4 m^*}{2(\epsilon_0 \epsilon_r)^2 \hbar^2} \frac{1}{n^2} \approx 10-60 \text{ meV}$$

→ fully ionized at moderate temperatures → Doping

$$a_n^* = \frac{\epsilon_0 \epsilon_r \hbar^2}{m^* e^2} n^2$$

$a_0 = 0.529 \text{ \AA}$ Bohr radius, $a_{\text{Si}} \sim 30 \text{ \AA}$; $a_{\text{Ge}} \sim 80 \text{ \AA}$

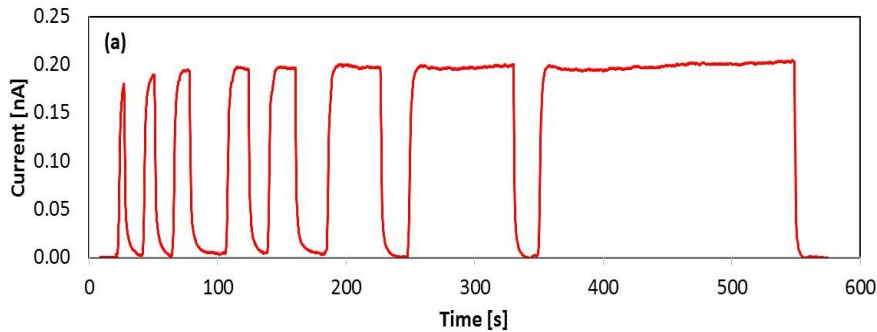
→ delocalized wave functions

$$E_n \propto -\frac{m^*}{\epsilon_r^2}$$



A level e.g. that in silicon is a few tens of meV reduces to few meV in CsPbBr₃ ($m^* = 0.13m_0$ and $\epsilon_r = 29.37$)

Polycrystalline: linear dependence of collected charge/current on adsorbed dose and dose rate



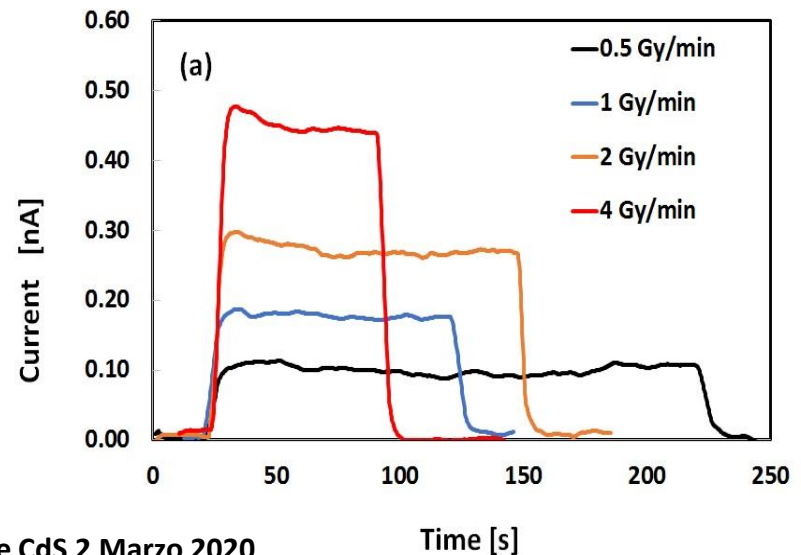
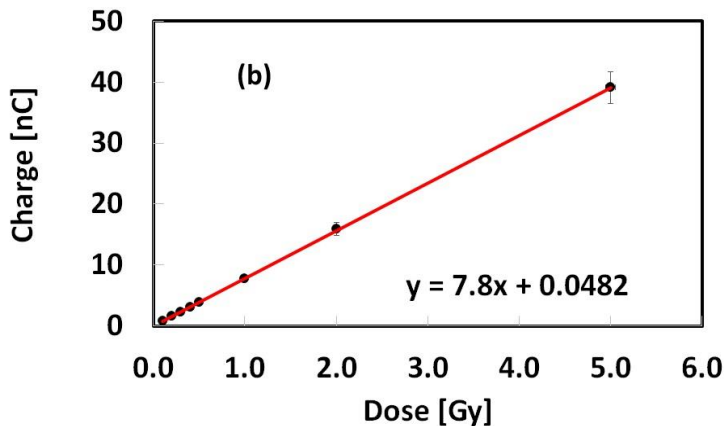
→ Active thickness reduced due to defects

$$S_{\text{CsPbBr}_3} \sim 70 \text{ nC} / (\text{Gy}\cdot\text{mm}^3)$$

$$S_{\text{Si}} = 637 \text{ nC} / (\text{Gy}\cdot\text{mm}^3)$$

$$S_{\text{air}} = 35 \text{ pC} / (\text{Gy}\cdot\text{mm}^3)$$

$$S_{\text{diam}} \sim 4 \text{ nC} / (\text{Gy}\cdot\text{mm}^3)$$



First proof-of-principle of inorganic perovskites clinical radiotherapy dosimeters

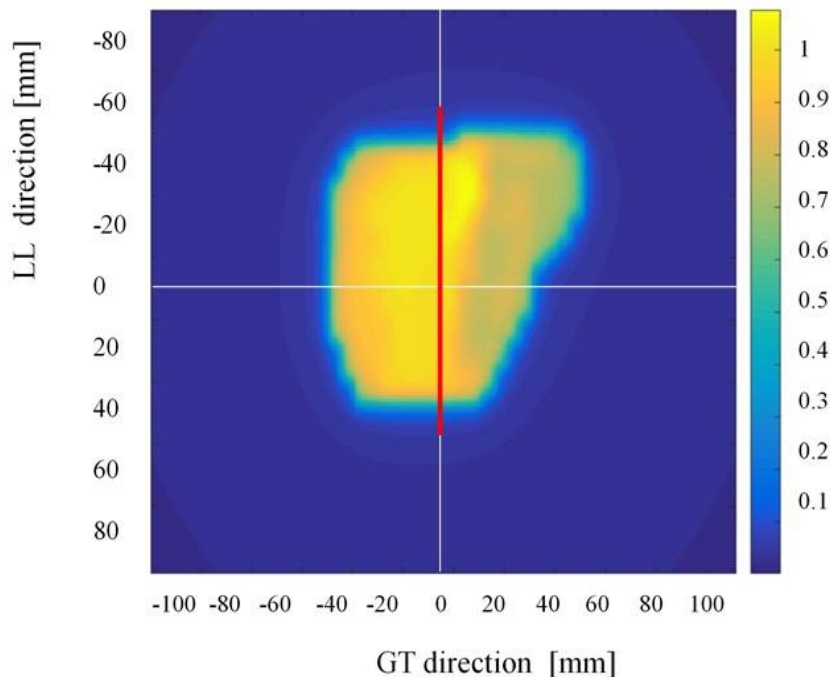
Cite as: APL Mater. 7, 051101 (2019); <https://doi.org/10.1063/1.5083810>
Submitted: 30 November 2018 . Accepted: 02 April 2019 . Published Online: 03 May 2019

Mara Bruzzi, Cinzia Talamonti, Nicola Calisi, Stefano Caporali, and Anna Vinattieri

M. Bruzzi, INFN Firenze CdS 2 Marzo 2020

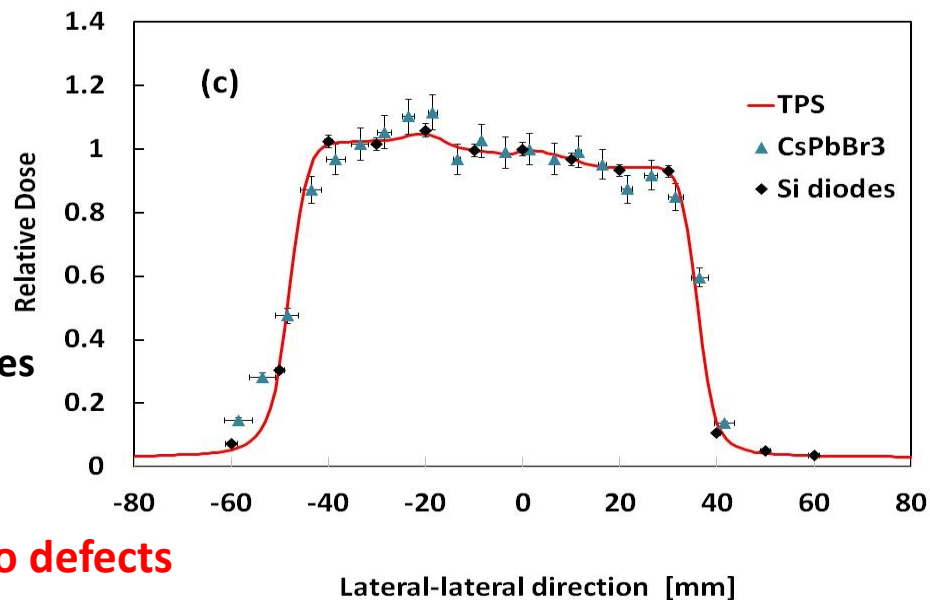
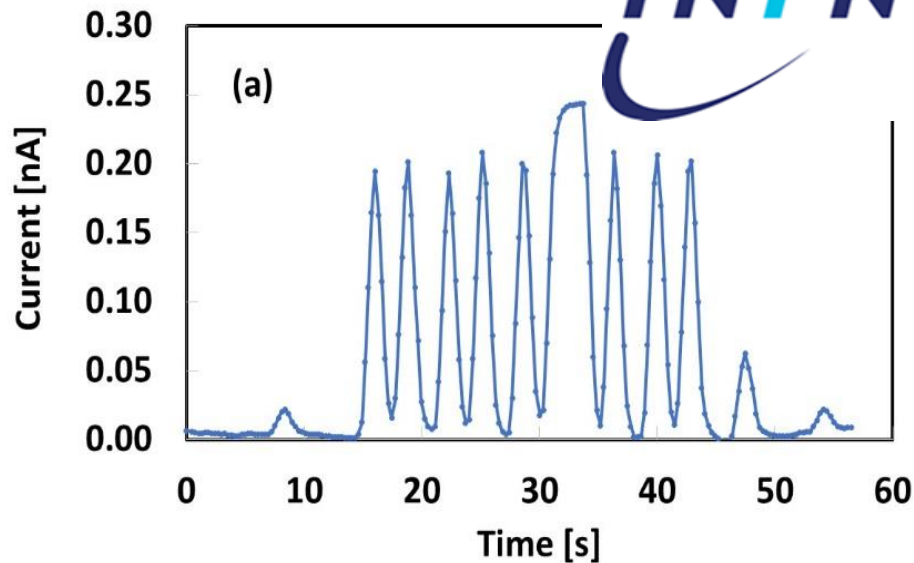
CsPbBr₃ : promising with IMRT beams;

Response comparable to silicon , but slower dynamics



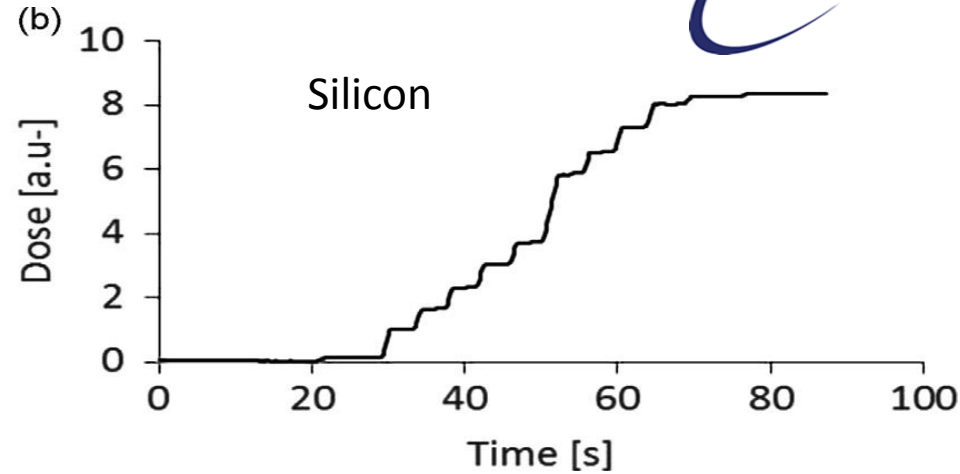
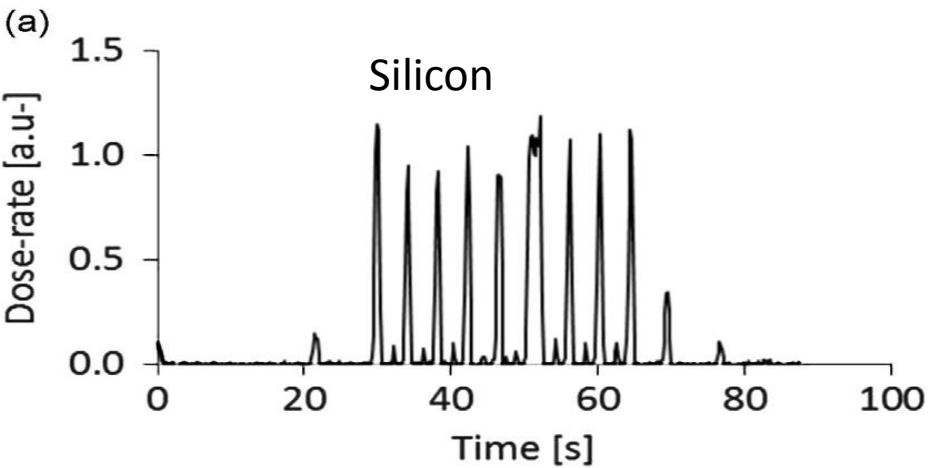
Bruzzi et al. APL Mater. 7, 051101 (2019);

TPS dose map for prostate cancer treatment
GT = Gantry Target direction; LL=lateral-lateral direction (isocenter at intersection red line evidences the profile measured with silicon and perovskite dosimeters)

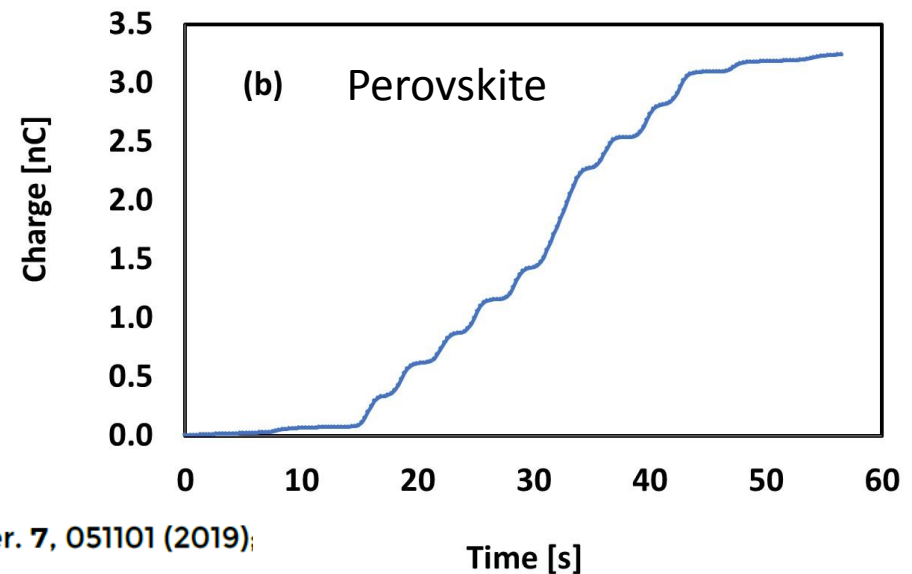
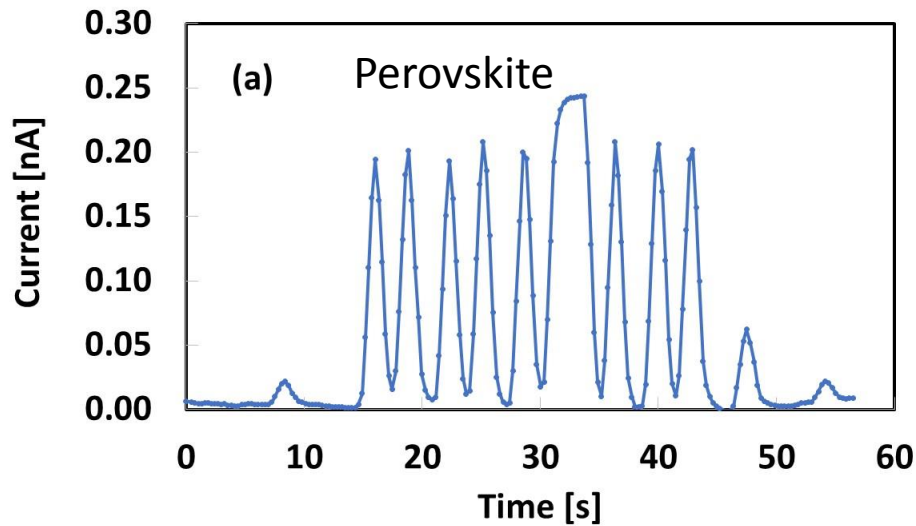


Open Issue → higher rise/decay times due to defects

Open issue: effect of native and radiation induced defects



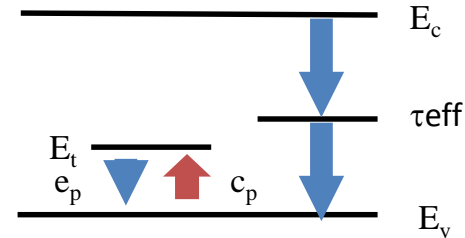
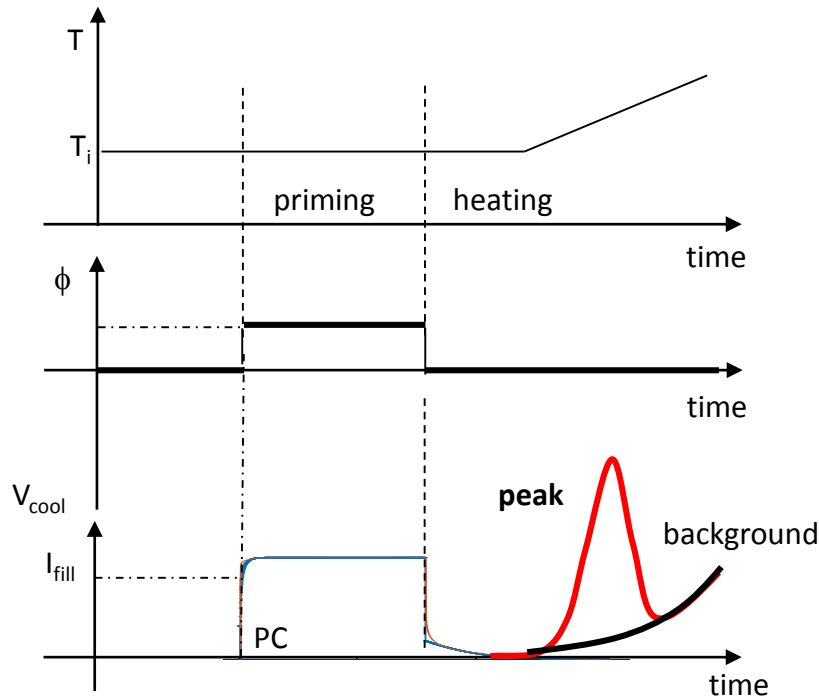
M. Bruzzi, NIMA 809, 2016 Novel Silicon Devices for Radiation Therapy Monitoring, 105-112



APL Mater. 7, 051101 (2019);

Slower rise/decay times when radiation switches. This effect should be minimized to increase dose measurement accuracy.

Thermally Stimulated Current (TSC) to reveal native and radiation induced traps



- V_{bias} applied
- Cooling to initial temperature T_i
- Filling traps with light source pulse
- heating at constant rate $\beta = dT/dt = \text{const}$
- cooling at constant rate

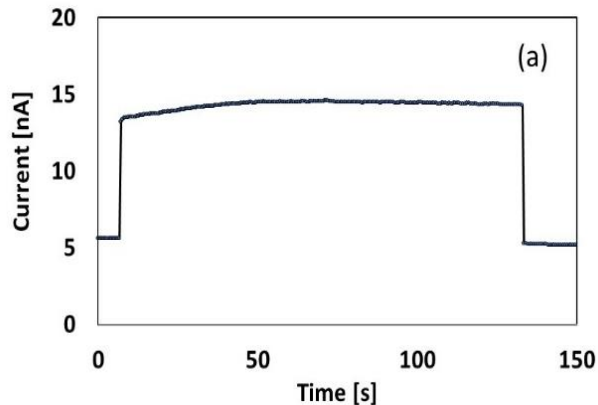
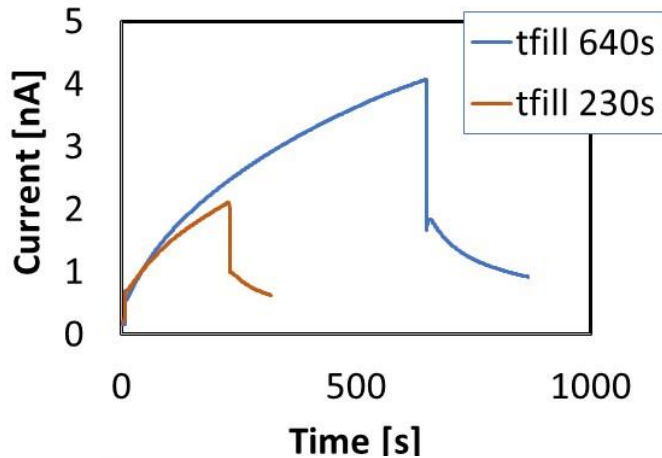
Thermally Stimulated Current:

- Peak due to charge emitted from trap only during heating;
- Background due to thermal generation rate, same during heating and cooling.

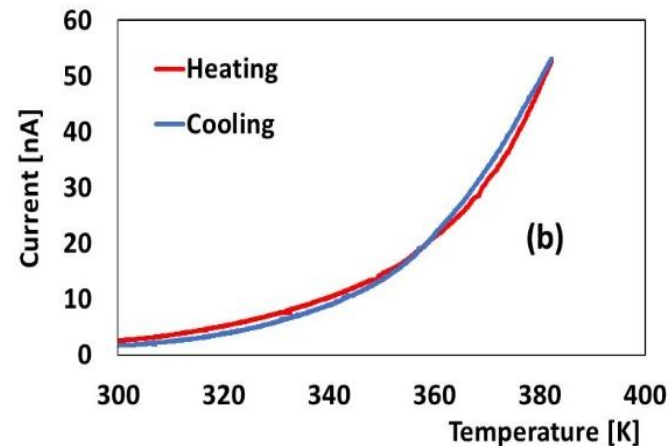
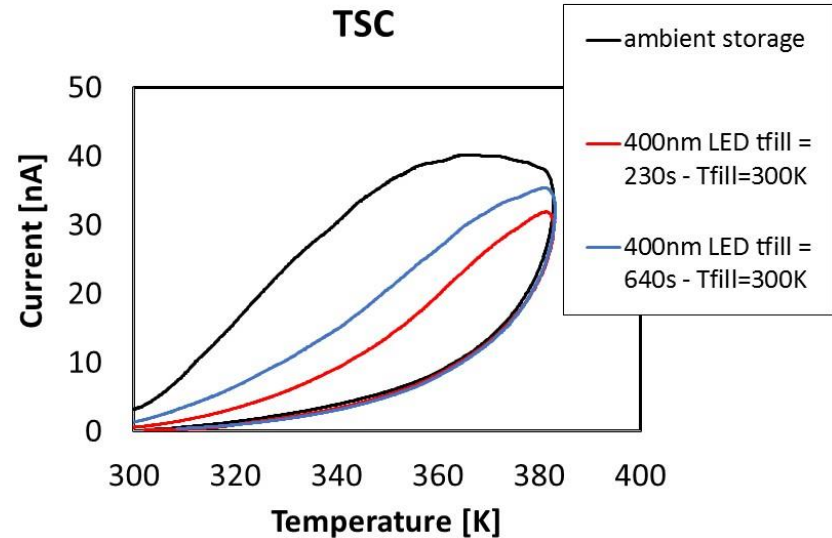
$$I_{TSC}(T) = e \mu_p F A \tau_{eff} p_{t0} e_p(T) e^{-\frac{1}{\beta} \int_{T_i}^T e_p(T) dT}.$$

New results: Main defect active at RT 0.45eV. Present only in polycrystalline samples

PC at 300K - 400nm LED



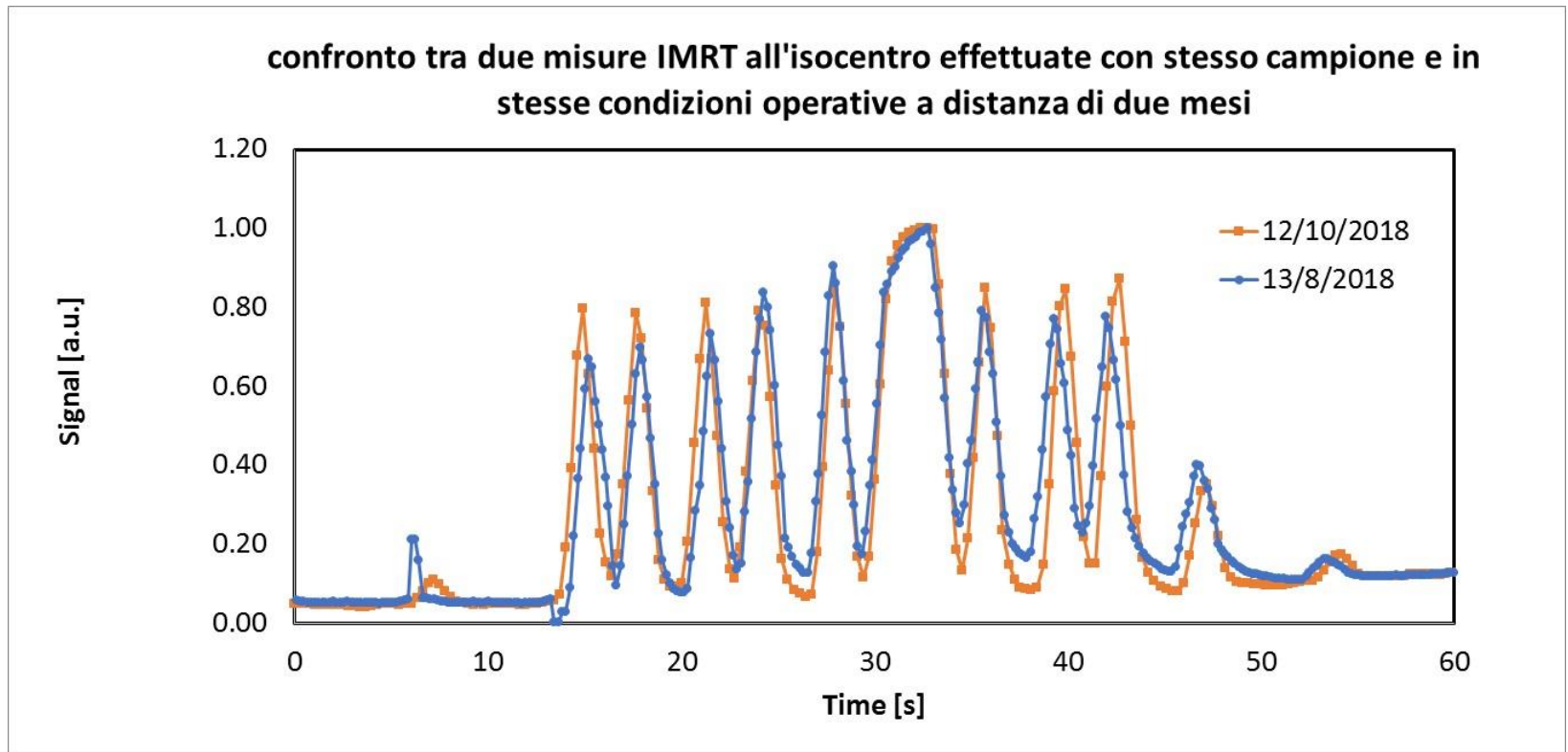
TSC



Mara Bruzzi, Naomi Falsini, Nicola Calisi, Anna Vinattieri, **Electrically active defects in polycrystalline and single crystal metal halide perovskite**, submitted to *Energies*, feb. 2020, section: Advanced Energy Materials, issue: Progress in Inorganic Halide Perovskites, Inorganic Perovskites

Open issues

- Reproducibility;
- Radiation Hardness;
- Single crystal performance under X-ray beam
- Schottky barrier devices to increase S/N



Conclusions

- Advanced imaging and dosimetry systems needed to get increased accuracy in radiotherapy treatment plans;
- State-of-art segmented detectors made with silicon (**epitaxial, Italian patent**)
- Diamond potentially best suited for X-ray radiotherapy due to energy independence of its response (tissue equivalence); segmented dosimeters not yet available commercially; **Florence prototype shows excellent performances under IMRT and VMAT treatment plans;**
- Volumetric dosimetry : **next generation of high sensitivity – flexible geometry systems** based on **perovskite materials** under development,
 - open issues: optimizing deposition techniques and device engineering, influence of defects on dosimetric properties, radiation hardness.